

Chapter IV

THE TNR RECEIVER

DOI	https://doi.org/10.25935/vps6-jb33
Publisher	MASER/PADC
Citation	Sitruk, L. & Manning, R. (2022) <i>The GGS/WIND/Waves Experiment</i> – Chapter 4 (Version 4.3, translated by A. Fave). MASER/PADC. doi:10.25935/VPS6-JB33
License	CC-BY-4.0

Summary

The Thermal Noise Receiver (TNR) is designed to analyse the quasi-thermal noise generated by the plasma electrons around the antenna. It consists of two analog sub-receivers, TNRA and TNRB, which perform signal pre-processing (automatic gain control, anti-aliasing filtering), and a fully digital module, TNRC. At each of the TNRA and TNRB sub-receivers, the signal is analysed in 5 frequency bands from 4 to 256 kHz. Then the signal in each band is analyzed by the TNRC using 16 or 32 digital filters with logarithmically distributed center frequencies. There is an octave of overlap between two successive frequency bands, so that the plasma frequency can be identified as accurately as possible. The spectral resolution of the instrument, given by the bandwidth of a digital filter, is equal to 4.4% of the centre frequency (case of 32 channels per band), i.e. 0.176 kHz to 11.264 kHz. Its time resolution is high: the integration time of a 16 or 32 point spectrum ranges from 1.472 s to 0.184 s. The signal spectrum is calculated on board, at the TNRC digital module, and a formal neural network, trained on the ground from ULYSSES/URAP data adapted to the particularities of the WIND/Waves receiver, determines the local plasma frequency. This information allows the DPU, in case the associated mode (tracking mode) is implemented, to be permanently located in the best adapted frequency band around the plasma frequency. The calculated data (16 or 32 spectrum values, plasma frequency, values around the plasma frequency) are transmitted to the DPU. The ground analysis of the thermal noise spectrum allows to determine both electron density and temperature, as well as solar wind speed and proton temperature.

Content

4 THE TNR RECEIVER.....	134
4-1 Thermal noise spectroscopy	134
4-2 Instrumental design	136
4.3. Frequency characteristics	139
4.3.1. Frequency bands	139
4.3.2. Frequency band splitting	140
4.3.3. Logarithmic frequency distribution.....	141
4-4 Instrument modes	144
4.5. How TNRC works.....	145
4.5.1. General operation.....	145
4.5.2. Acquisition	145
4.6. Digital filtering.....	146
4.6.1. Position of the problem.....	146
4.6.2. Classic method	147
4.6.3. Method used.....	149
4.6.4. Other reductions.....	150
4.7. Spectra and AGC integration times.....	151
4.7.1. Integration times.....	151
4.7.2. Consideration of the integration period	153
4.7.3. Data compression	154
4.7.4. Communication TNR-DPU	155
4.8. Learning process	158
4.8.1. Principle	158
4.8.2. Pre-treatment.....	158
4.8.3. NN Characteristics and Learning	159
4.8.4. Remarks	161
4.9. Estimation of the parameters f_p, T_c, α, τ	163
4.9.1. Digital adjustment.....	163
4.9.2. Cubic interpolation	165
4.10. Ground data transmission.....	166
4.10.1. Transmitted data from TNR to DPU.....	166
4.10.2. Data transmitted by the DPU to the telemeter	167
4.11. Scanning of frequency bands	170
4.11.1. The different scanning modes.....	170
4.11.2. The pursuit mode.....	170
Remarks	172

4 THE TNR RECEIVER

4-1 Thermal noise spectroscopy

The thermal motion of ions and electrons passing near a passive electric antenna in contact with a plasma generates plasma waves. These waves are emitted near the fundamental frequency of the medium, the so-called plasma frequency¹ f_p , and produce electrical potential fluctuations (electrostatic fluctuations) at the antenna, or thermal noise². The TNR receiver measures the power spectrum of the potential difference across the antenna. This spectrum has the following form:

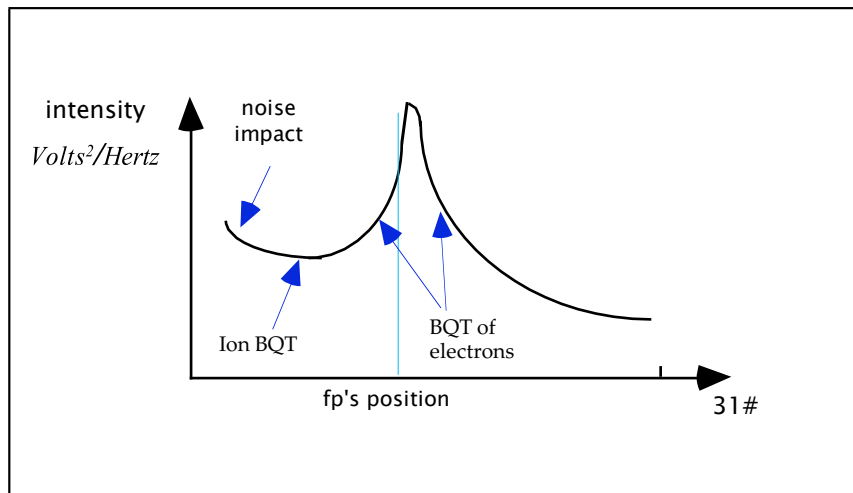


Fig. Thermal noise spectrum

The fluctuations of the electrostatic field are completely determined by the electron velocity distribution function (*Rostocker, 1961*). These fluctuations are therefore a source of information on the different moments of this function in the ambient plasma. The theoretical expression of the measured spectrum was obtained by assuming a Maxwellian model: the velocity distribution function is described as the sum of two Maxwell ("maxwellian")³ distributions representing i) the "cold" electrons, of density and temperature N_c, T_c (core), and 2) the population of suprathermal⁴ ("hot") electrons, of density and temperature N_h, T_h (halo). The numerical fitting of the real spectra to this model allows to determine the values of the four parameters⁵ N_c, T_c, N_h, T_h (see § 4-9 and appendices). The low frequency part of the spectrum preceding the peak corresponds to the

¹ The plasma frequency acts as a cut-off frequency for the medium: electromagnetic waves with frequencies lower than f_p cannot propagate (evanescent waves).

² or Quasi-Thermal Noise (QTN) since two electron distributions are considered. This original plasma diagnostic technique, initiated in the framework of the ISEE3 experiment, is due to N. Meyer-Vernet et al. at DESPA, who designed and modelled it. The theoretical calculation and computer implementation are nothing less than trivial, see appendices.

³ Cf. glossary

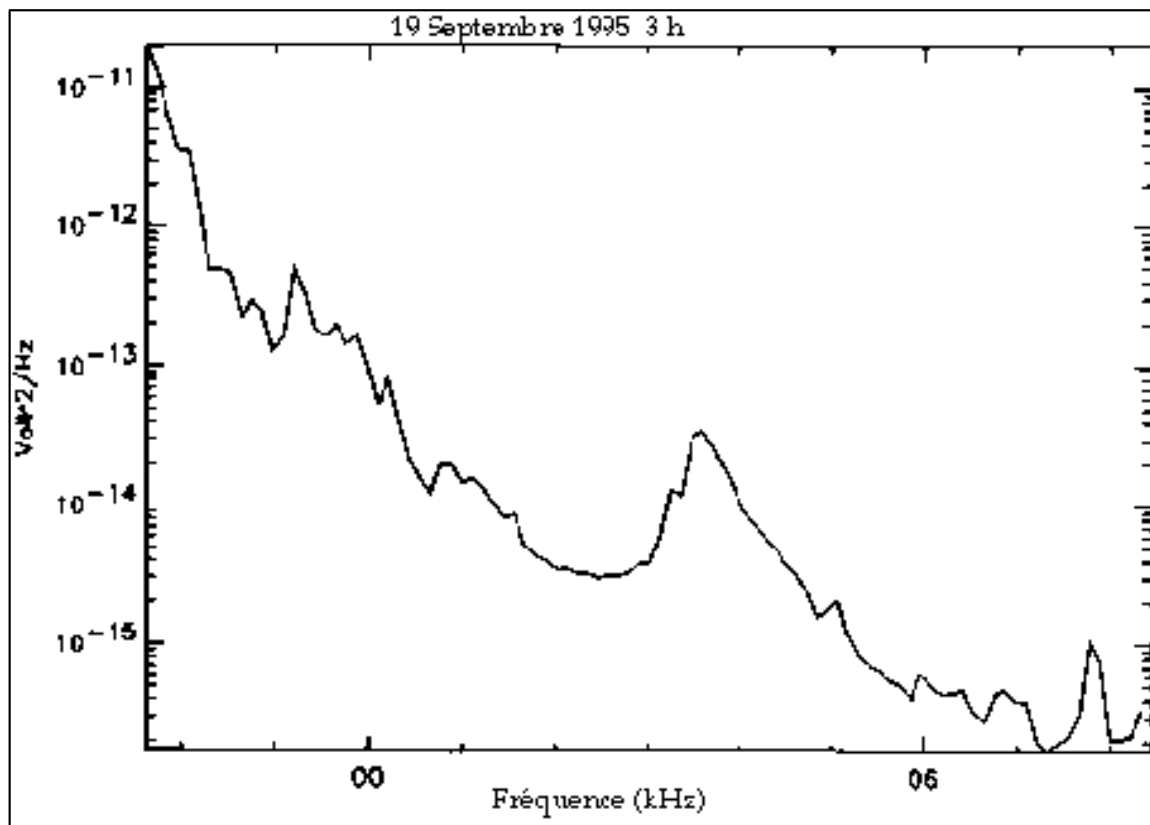
⁴ Note that electrostatic particle analyzers provide accurate measurements of the moments (density, temperature, velocity) of suprathermal electrons.

⁵ The possibility of deducing the solar wind speed is also being investigated [ISS].

impact noise of electrons and ions on the antenna⁶, to the photo-electron emission due to solar radiation, and to the ion contribution to the thermal noise, shifted by the Doppler effect by the solar wind speed. This last contribution allows to calculate the overall solar wind speed and the proton temperature. The density, the temperature and speed are basic parameters for understanding the structure of the solar wind and its interaction with the magnetosphere.

Let us briefly recall the characteristics of this method (see the appendix for more details):

- It provides several essential parameters of the plasma: density and temperature of electrons. The extension of this method to the determination of the solar wind speed and the proton temperature is under study.
- It could be implemented in various space environments: solar wind, cometary ionosphere, planetary.
- It does not disturb the plasma: it is a passive "diagnostic" method.
- It is relatively insensitive to the photoelectrons generated by the satellite.
- It does not require fine calibrations for density, unlike temperature or velocity⁷.
- It is optimal for cold and dense plasmas.
- It is best suited to thin, wire antennas longer than the Debye length of the medium.
- As it measures a weak signal, it requires a quality EMC.
- It requires sufficient frequency resolution at the spectral peak.
- Its results can be compared with the results of other in situ analysers (waves, ions, electrons) on the same satellite.



Example of a thermal noise spectrum

⁶ The impact of electrons and ions on the antenna can, depending on the exposed surface, have a significant effect on the signal. The spectral contribution to the impact noise is a very steep negative slope for frequencies below 10 kHz.

⁷ For high solar wind speeds, the fitting of thermal noise spectra is unsuccessful. However, removing these spectra from the database introduces a bias in the study of the other parameters (in particular the temperature). On the contrary, taking into account the solar wind speed as a fitted parameter has allowed to increase the number of spectra that can be fitted and to refine the analysis of the other parameters.

Note: The frequency range of the TNR instrument could also allow the study of the Galactic radio frequency spectrum. Such a study is under consideration.

4-2 Instrumental design

The TNR instrument consists⁸ of two analogue receivers TNRA, TNRB and a digital receiver TNRC. Schematically, it is presented as follows (see also the detailed diagram):

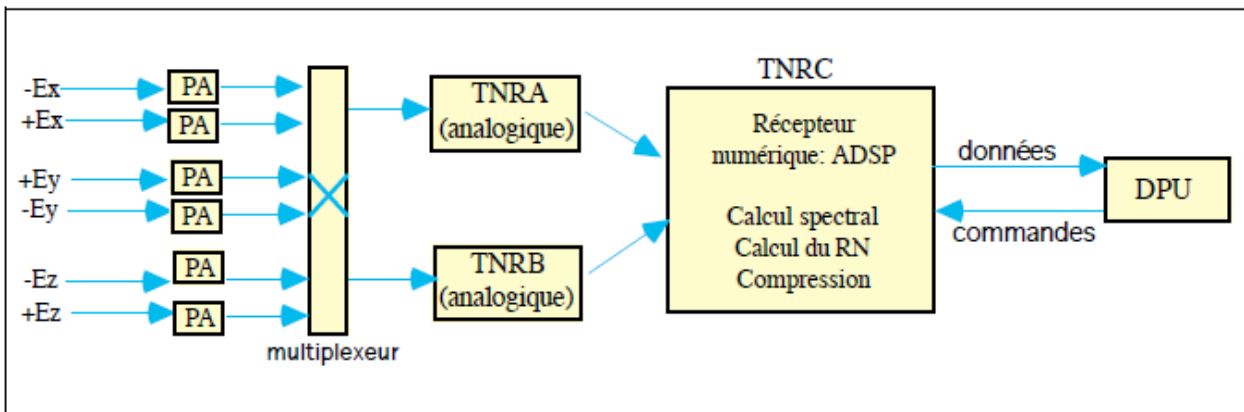


Fig. Simplified schematic of the TNR receiver

The two analogue receivers TNRA and TNRB each acquire, via a multiplexer, the measurements of one of the three electrical antennas. The possible antenna combinations are as follows⁹:

	TNRA	TNRB
Combination 1	E_x	E_y
Combination 2	E_x	E_z
Combination 3	E_y	E_x
Combination 4	E_y	E_z

Combination 1 is the default antenna combination¹⁰, i.e. the one in effect immediately after a "Power on" (the first time) or a "Reset" (during a mission). The other combinations can be remotely controlled (AC). It can be seen that the TNRA receiver can be connected to E_x or E_y , and that the TNRB receiver can be connected to E_x , E_y or E_z .

- The analogue signals pass through the TNRA and TNRB analogue receivers, which pre-process the signal using anti-aliasing filtering¹¹ and Automatic Gain Control (AGC). The latter circuit includes a

⁸ One module for TNRA, one module for TNRB, one module for TNRC.

⁹ Two control bits are available (in the DPU) for the two antennas, which allow 4 combinations to be coded (00, 01, 10, 11).

¹⁰ The TNRA receiver is intended especially for thermal noise analysis. It is by default connected to the E_x antenna, which is a long antenna and therefore best suited to the frequency range [4 kHz, 256 kHz] of the TNR. The TNRA receiver was therefore deliberately set to be more sensitive than the TNRB receiver (which has a higher saturation level). It turns out that this was not the case in practice (cf. § calibrations).

¹¹ Elimination of frequency components beyond the highest limit of the desired frequency band, see glossary. In the present case, "active filters" are used (operational amplifier based circuit) to obtain a very good rejection. This type of circuit avoids the high order succession of Resistor/Capacitor stages.

logarithmic amplifier whose gain adjusts automatically according to the level of the input signal, which allows intense events to be taken into account. It outputs the amplified input signal with a constant, rapidly changing RMS level (waveform), as well as the slowly evolving AGC signal, which is related to the gain of the amplifier¹². The principle of an AGC amplifier¹³ (logarithmic feedback) has been described in the context of RAD1/2 instruments, except that here both signals at the output of this circuit are considered: the waveform signal and the AGC level.

The TNRA/B receivers each contain 5 sub-receivers in parallel corresponding to each of the 5 frequency bands¹⁴ A, B, C, D, E of TNR. Each frequency band consists of 16 or 32 channels (= 16 or 32 digital filters). The frequency characteristics of the TNR are described in the following paragraph.

The AGC signal and the waveform signal from each of these 5 sub-receivers are coded to 8 bits by an extremely fast flash analog-to-digital (A/D) converter ("flash"), which can acquire more than $2 \cdot 10^7$ samples per second.

- A digital subassembly TNRC then collects the results of TNRA or TNRB or both, each through an A/D converter. The TNRC is a microprocessor-based module¹⁵ ADSP 2100. It has been programmed to perform spectral analysis of the signals and automatically recognize the position of the plasma line from a spectrum calculated during the mission. This is the first fully digital instrument built at DESPA. This digital filtering is of the same type as those used on the TSS (RETE receiver), CLUSTER (STAFF receiver) and CASSINI (RPWS receiver) missions.

The total dynamic range of the TNR, which is close to 100 dB, is determined by the sum of the dynamic range of the analogue part: 70 to 80 dB, and the digital part¹⁶, the latter being determined by the dynamic range of

the A/D converter: $20 \log_{10} \left[\frac{(2^8 - 1)}{2^0} \right] = 48 \text{ dB}$ (actually a little less, see above).

The DPU controls the operation of the TNR: it selects the antennas, the frequency band, and the mode.

The on-board computer memory of the TNR instrument consists of 12 kB of read-only memory (ROM)¹⁷, and 48 kB of random access memory (RAM). About half of the RAM is not used by the on-board software initially: a significant part of it remains available for possible downloading of additional instructions and coefficients.

¹² This is referred to as an AGC circuit, and the AGC value is the output of the AGC circuit giving the control voltage for the variable gain amplifier.

¹³ In practice, two AGC circuits are cascaded to achieve the required high dynamic range of 80 dB (40 dB for each stage).

¹⁴ An AGC circuit¹⁴ is designed to operate in a certain frequency range because its response time varies approximately as $1/f$ min. Therefore, there is an AGC circuit associated with each frequency band of the TNR.

¹⁵ The ADSP 2100 microprocessor is a space-qualified RISC CMOS signal processor or DSP designed by Analog Devices.

¹⁶ An AGC circuit operates within a limited range of input signal amplitude. If the signal at the input of the analogue circuit becomes too low, the AGC circuit is no longer able to provide an adequate response and amplifies the signal to the maximum; the digital circuit (the A/D converter) then takes over the dynamic range and continues to code the signal. It is always possible to reconstitute the signal at the analog input, knowing the value of the AGC and the coding of the waveform by the A/D unit. This A/D relay implies that the dynamics of the analog and the digital are added together. Indeed, a signal between the amplitudes $V1$ and $V3$, and let $20 \log(V3/V2)$ be the dynamics of the analog circuit (with $V1 < V2 < V3$), and $20 \log(V3/V1)$ the dynamics of the digital circuit. We have $20 \log(V3/V1) = 20 \log(V3/V2) + 20 \log(V2/V1)$. TBV. Recall that the dynamic range of a circuit is (in dB) the ratio between the highest and lowest amplitude signal it can detect.

¹⁷ The ADSP code and coefficients fit in 12 kB of memory.

We have the following comparison table (TBC) for example for the WIND/TNR, ISEE-3/ICE/SBH, ULYSSE/URAP experiments:

Mission/Receiver	Frequency and time characteristics
WIND/TNR	<p>48 or 96 channels from 4 to 256 kHz.</p> <p>Frequency resolution of $f = 9\%$ or 4.4% of f_c, i.e.: 0.36 kHz to 23.04 kHz or 0.176 kHz to 11.264 kHz</p> <p>Time resolution: 0.184 s to 1.472 s for spectrum acquisition. Recall: 256 channels from 20 to 1040 kHz (RAD1). 256 channels from 1075 to 13825 kHz (RAD2).</p>
ISEE-3 /ICE/SBH	<p>Frequency range from 30 kHz to 2 MHz: two radiometers each scan a different set of 12 frequencies. Frequency resolution of the radiometers: 10 kHz and 3 kHz.</p> <p>Time resolution: time required to acquire a spectrum: approx. 1 min. (TBC)</p>
ULYSSE/URAP	<p><u>Two-channel low-frequency receiver</u> ("RAR low"): Using a frequency synthesizer, linear scanning of 64 low-frequency channels (1.25 kHz to 48.5 kHz), bandwidth 0.75 kHz, equally spaced, each step 2 s long, thus covering the frequency range in: $64 \times 2 \text{ s} = 128 \text{ s}$. Thus we have:</p> <p>$1.25 \text{ kHz} + n \cdot 0.75 \text{ kHz}$ with $n = 0$ to 63.</p> <p>Frequency resolution: 0.75 kHz. Time resolution: 128 seconds for the acquisition of a spectrum.</p> <p>Receivers connected to the dipole antenna located in the plane of rotation or to the sum of the signals of the rotation plane antenna and the axial antenna.</p> <p><u>Two-way high frequency receiver</u> ("RAR high"): 12 high frequency channels: 52, 63, 81, 100, 120, 148, 196, 272, 387, 540, 740, 940 (kHz). by quartz oscillator.</p> <p>Frequency resolution: 3 kHz. Time resolution: 144 seconds Receivers connected to the rotation axis monopole</p>

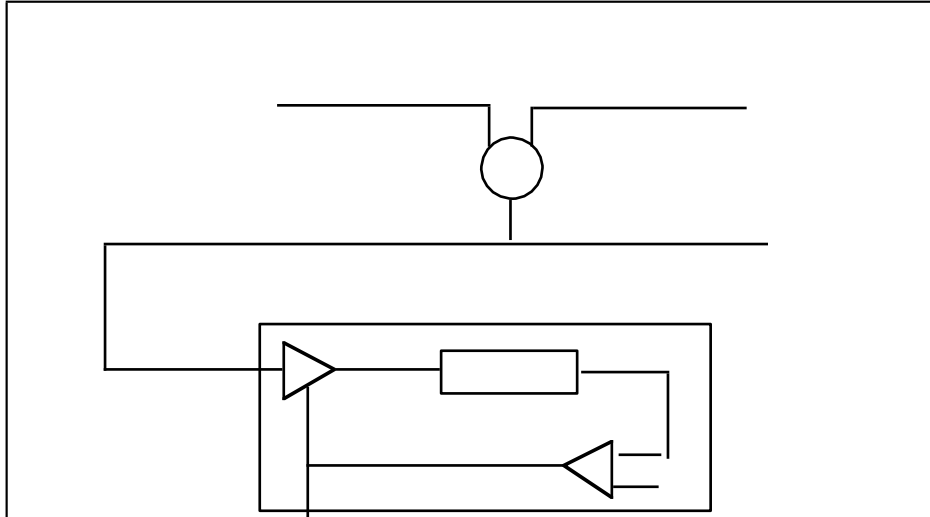


Fig. block diagram of the TNR instrument

4.3. Frequency characteristics

4.3.1. Frequency bands

The frequency range covered by the TNR instrument is from 4 kHz to 256 kHz. This range consists of 5 frequency bands, denoted A, B, C, D, E. Each frequency band consists of 16 or 32 digital filters whose centre frequencies are logarithmically distributed (see above). A frequency band covers two octaves¹⁸ in frequency and there is an octave of overlap between two consecutive frequency bands. This large overlap is designed to capture the plasma frequency: changing frequency bands in effect refocuses a spectrum that would be off-centre at a given time and in a given band.

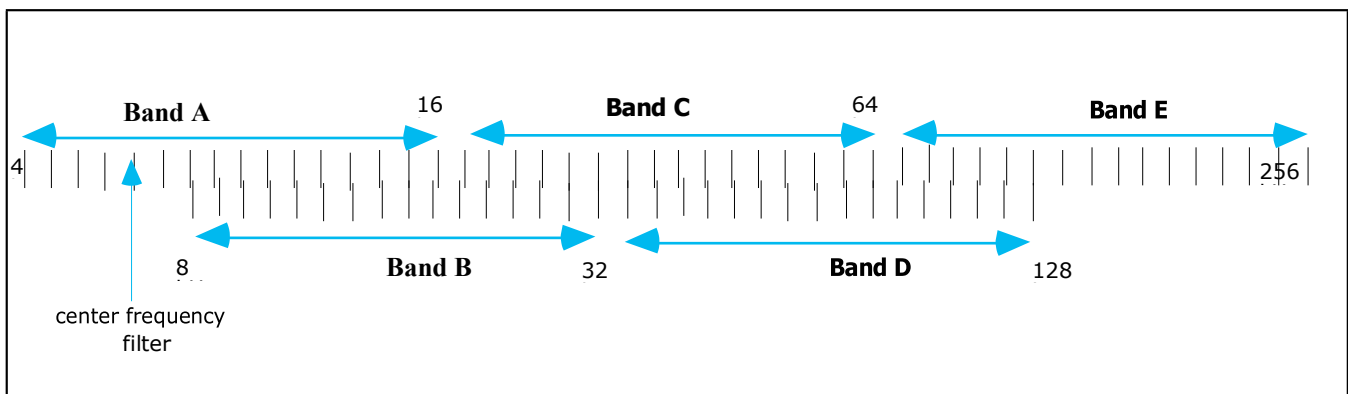


Fig. Logarithmic scale diagram of TNR filter center frequencies (case of 16 filters per band).

The frequency ranges of the different bands and the associated sampling frequencies are as follows:

	Frequency range (kHz)	Frequency range (kHz)
Band A	4 - 16	64.1
Band B	8 - 32	126.5

¹⁸ The frequency interval between a frequency f and its double: $[f, 2f]$. In band A, for example, an octave covers the range 4 to 8 kHz.

Band C	16 - 64	255.7
Band D	32 - 128	528.5
Band E	64 - 256	1000

To change the frequency band, it is sufficient to change the sampling frequency¹⁹ at the C A/N and also to control the analogue circuit accordingly.

4.3.2. Frequency band splitting

The choice of a single frequency band covering the entire frequency range available at the output of the antennas is not optimal. This range must be broken down into several frequency bands, in this case the five bands A, B, C, D, E. The explanation is as follows:

- The relationship between the order of a filter (the number of its coefficients), its frequency width f , and the sampling frequency f_{ech} , is written (see § 4-5-2):

$$ordre = c^{te} \cdot \frac{f_{ech}}{\Delta f} \quad (1)$$

However, the digital filters of the TNR instrument are designed in such a way that we have (see above):

$$\Delta f / f_c = c^{te}$$

So that at low frequencies: f_c low, the filters are very narrow: Δf low.

If, in addition, a high value of f_{ech} is chosen, relation (1) shows that the order at low frequency is likely to be high²⁰, which is not desirable, for reasons of computational speed and limitation of the number of coefficients stored in memory.

A too high sampling frequency f_{ech} therefore limits the frequency resolution Δf at low frequencies. It is therefore advantageous to divide the frequency range into several frequency bands (of two octaves here), which avoids having the same sampling frequency for the entire range.

- The lower the sampling frequency, the more the anti-aliasing filter will have to be characterized by a strong rejection to limit the signal spectrum. Indeed, the latter extends in practice over all frequencies, and the phenomenon of frequency aliasing must be avoided. However, it turns out that a high rejection filter is difficult to achieve in practice.

¹⁹ At rest, the C A/N does not sample the signal ($f_{ech} = 0$). To make the C A/N unit sample the signal, the ADSP generates a logic signal with a frequency equal to the sampling frequency: 64 kHz, 126 kHz, etc. On each rising edge of the signal transmitted by the ADSP, the C A/N samples the signal.

²⁰ Consider the following extreme case: if there were only one frequency band from 4 to 256 kHz, and if the sampling frequency of the E-band was kept at $f_{ech} = 1000$ kHz for the whole range, then, for the lowest centre frequency $f_c = 4$ kHz and in the case $\Delta f / f_c = 0,044$, a filter length (taking 1.3 for the constant) of $1,3 \cdot 1000 / (0,044 \times 4) = 7386$ which represents a considerable number of coefficients for a single filter.

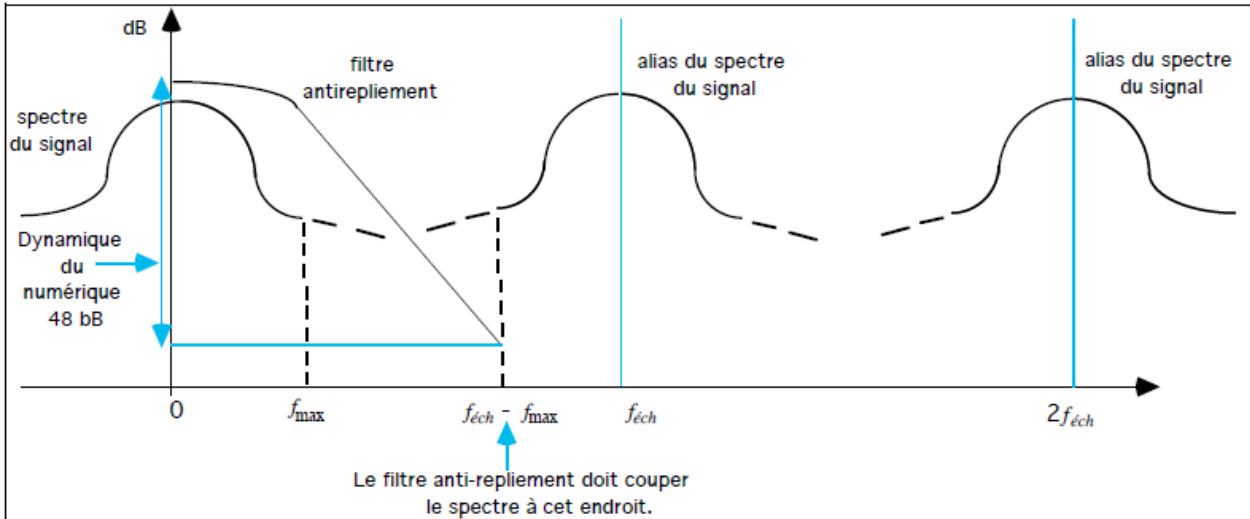


Fig. Anti-aliasing fitment

Since the dynamic range of the TNRC is limited to 48 dB, the anti-aliasing filter must cut the frequencies of the spectrum so that it has a dynamic range of 48 dB at the output of the analog part (see diagram).

This constraint, which is antinomic to the previous one, forces a compromise. For this experiment, the sampling frequency is chosen to be about four times the maximum frequency in the band, as can be verified for each frequency band (table § 4-3-1), whereas the sampling theorem²¹ only requires a ratio of two.

4.3.3. Logarithmic frequency distribution

The filters are designed in such a way that we have $\Delta f / f_c = c^{te}$, Δf being the bandwidth at 3 dB, designed to be also the distance between the center frequencies of the filters²². The result is that as the frequency increases in a band, the bandwidths Δf of the filters become larger and the centre frequencies f_c of the filters become more widely spaced, as can be seen in (figure). The solution of the recurrent equation²³:

$$\frac{f_c(i+1) - f_c(i)}{f_c(i)} = c^{te}, \quad 0 \leq i \leq n-1,$$

with the boundary conditions of the band: $f_c(0) = f_{c,\min}$ et $f_c(n) = f_{c,\max}$ (minimum and maximum frequencies in the considered band), leads to the following expression:

$$f_c(i) = f_{c,\min} \left(\frac{f_{c,\max}}{f_{c,\min}} \right)^{i/n} \quad 0 \leq i \leq n, \quad n = 16 \text{ ou } 32$$

²¹ Still called Nyquist or Shannon or Witterker-Shannon theorem.

²² The ratio $\Delta f / f_c$ is related to the ratio $\lambda / \Delta \lambda$, which is by definition the spectral resolution of a spectrometer, of which it is a basic characteristic [LEN97]. We have: $\lambda / d\lambda = -f / df$.

²³ Or $f_c(i+1) / f_c(i) = c^{te}$, or else $\log(f_c(i+1)) - \log(f_c(i)) = c^{te}$, these formulations being equivalent.

Note. The above formula with $0 \leq i \leq n$ generates $n+1$ frequencies: only the first $0 \leq i \leq n$ are retained, the last centre frequency of a band and the first centre frequency of the following band being distant from Δf .

However, for the TNR frequency bands, the band ratio $f_{c,max} / f_{c,min}$ is always 4, regardless of the ($16/4 = 32/8 = 64/16 = 128/32 = 256/64 = 4$), hence:

$$f_c(i) = f_{c,min} \cdot (4)^{i/n} \quad 0 \leq i < n, \quad n = 16 \text{ ou } 32$$

The expressions for the center frequencies of the filters are therefore as follows:

<i>Cas 16 canaux</i>	$f_c(i) = f_{c,min} \cdot (2)^{i/8}$	$0 \leq i < 16$
<i>Cas 32 canaux</i>	$f_c(i) = f_{c,min} \cdot (2)^{i/16}$	$0 \leq i < 32$

With $f_{c,min}$ taking the values: 4 kHz, 8 kHz, 16 kHz, 32 kHz, 64 kHz.

This gives a logarithmic distribution of the centre frequencies. If we make explicit the values of $f_{c,min}$, by numbering the bands from 0 to 4, we can also write:

<i>Cas 16 canaux</i>	$f_c(i) = f_{c,min,bandeA} \cdot 2^j \cdot 2^{i/8}$	$0 \leq i < 16$	<i>et</i>	$0 \leq j \leq 4$
<i>Cas 32 canaux</i>	$f_c(i) = f_{c,min,bandeA} \cdot 2^j \cdot 2^{i/16}$	$0 \leq i < 32$	<i>et</i>	$0 \leq j \leq 4$

The exact list of these frequencies for 16 or 32 frequencies is given in Appendix I, in the case of 16 or 32 frequencies.

The type of distribution chosen for the centre frequencies therefore leads to the following frequency resolutions:

<i>Cas 16 canaux</i>	$\frac{\Delta f}{f_c} = \frac{f_c(1) - f_c(0)}{f_c(0)} = (2)^{1/8} - 1 = 0,09$	<i>soit</i> $\Delta f = 9\% \text{ de } f_c$
<i>Cas 32 canaux</i>	$\frac{\Delta f}{f_c} = \frac{f_c(1) - f_c(0)}{f_c(0)} = (2)^{1/16} - 1 = 0,044$	<i>soit</i> $\Delta f = 4,4\% \text{ de } f_c$

Taking into account the overlapping of the frequency bands, and the coincidence of part of the central frequencies from one band to the next (8 central frequencies coincide in the case of 16 filters/band, 16 in the case of 32 filters/band) - see the TNR channel diagram in § 4-3-1 -, there are therefore $3 \cdot n$ ($n = 16$ or 32):

48 or 96 different channels from 4 to 256 kHz, out of a total of $5 \cdot n$ ($n = 16$ or 32) i.e. 80 or 160 channels.

Remarks

- We have established experimentally the relation

$$\Delta f_{efficace} = 1.1 \cdot \Delta f_{3dB}$$

But $\Delta f_{3dB} = 0.09 \cdot f_c$ (case 16 filters) or $\Delta f_{3dB} = 0.044 f_c$ (case 32 filters)

We have therefore:

$$\Delta f_{efficace} = 0,099 f_c \quad (\text{cas 16 filtres})$$

$$\Delta f_{efficace} = 0,0484 f_c \quad (\text{cas 32 filtres})$$

- To avoid a problem of saturation in 0 and 255 during the digitization of the signal, the coding of the signal is carried out on a more restricted interval [i, j] with $0 < i$ and $j < 255$: it results that the dynamics of C A/N

is about 45 dB, not $48 \text{ dB} = 20 \log_{10} \left(\frac{2^8 - 1}{2^0} \right)$ the value that would have been obtained if we had used over the whole range [0, 255]. It is this dynamic range of the C A/N that ultimately limits the dynamic range of the digital filters, expressed by their rejection rate, which must therefore be less than 45 dB. In practice, this is more like 50 dB (a few dB are gained due to the noise of the digital part).

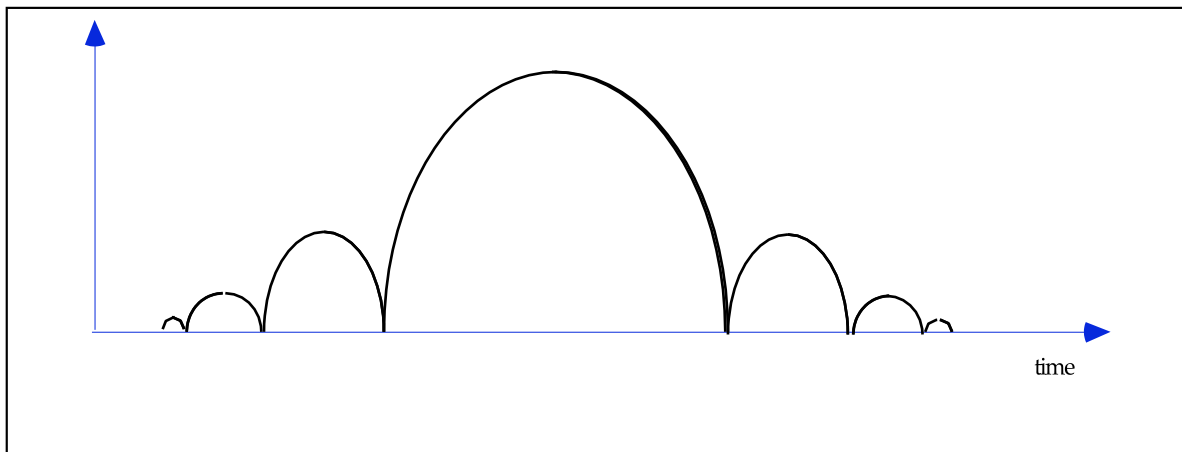


Fig. Diagram of the coefficients of the digital filters of the TNR instrument. Time domain. case of 16 filters (to be corrected --> real values)

Filtres numériques de l'instrument TNR: réponse en fréquence

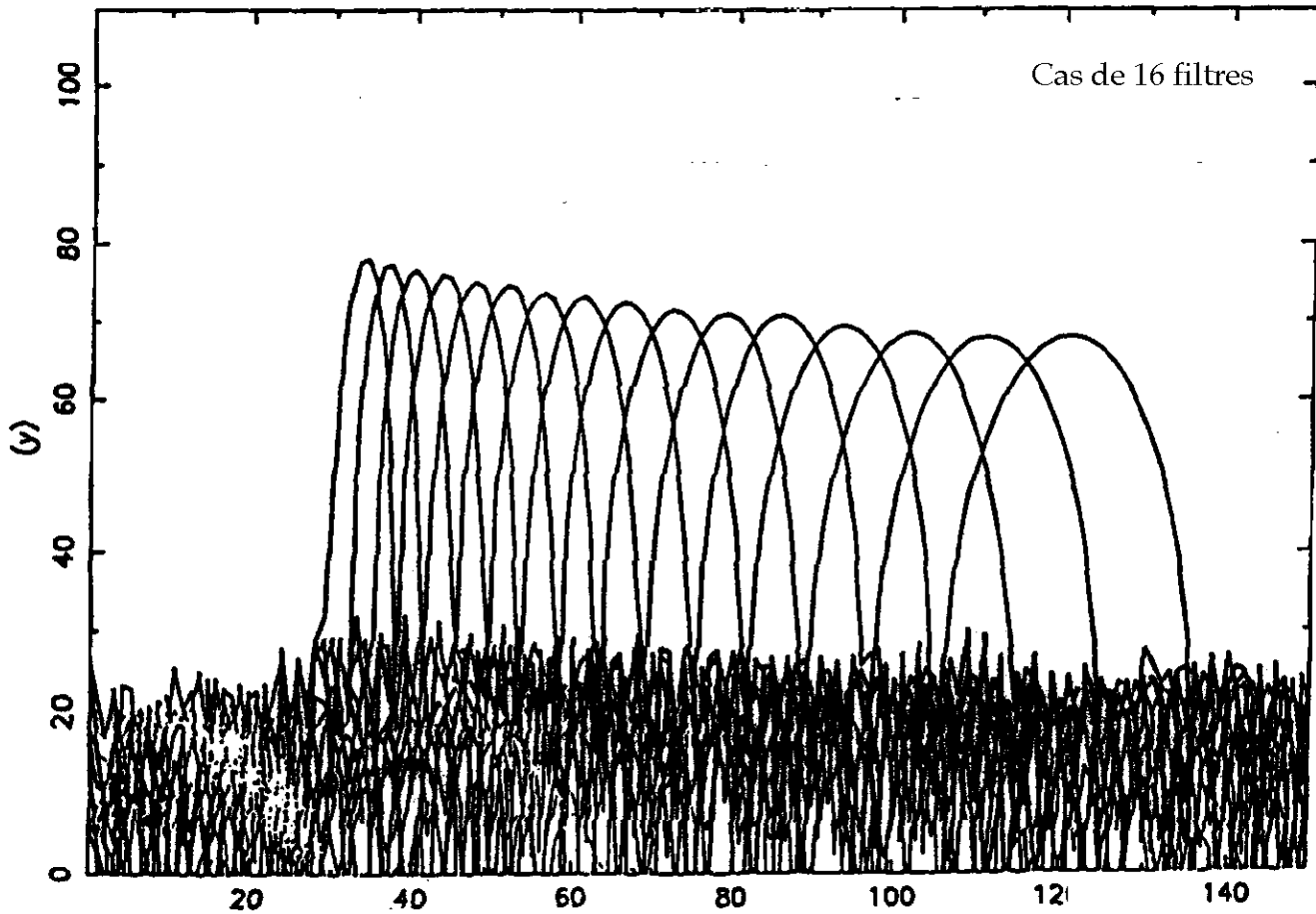


Fig. Diagram of the digital filters of the TNR instrument. Spectral domain.

4-4 Instrument modes

There are 5 possible modes of operation of the TNR:

TNR mode	Number of frequencies per spectrum	receiver(s) read
0	16	TNRA
1	16	TNRB
2	32	TNRA
3	32	TNRB
4	16	TNRA (16 freq.) and TNRB (16 freq.)

Mode 2 is the default mode.

4.5. How TNRC works

4.5.1. General operation

The operation of the TNRC module is shown in the flowchart in § 4-7-4. The DPU commands the TNR to perform processing for a given frequency band. The TNRC acquires 256 (or 512) samples of the signal, as well as an AGC value (or two, if in mode 4). Then the ADSP microprocessor performs a real time digital filtering, which allows the calculation of the successive spectra of the signal over time (see appendix). The results of these calculations, coded on 32 bits (TBC), are compacted to be transmitted to the telemetry. The 16 or 32 values of the successive spectra are also applied as input to a formal Neural Network (NN) which calculates the value of the associated plasma frequency f_p , as well as a confidence index of this choice. The spectrum, the AGCs, and the results of the RN are then transmitted to the DPU.

All these steps are explained in detail in the following paragraphs.

4.5.2. Acquisition

In general, the time window width ΔT of a filter and its bandwidth Δf are inversely proportional²⁴, and it can be written²⁵:

$$\Delta f \cdot \Delta T = \Delta f \cdot (\text{ordre} \cdot \text{période d'échantillonnage}) = \frac{\Delta f \cdot \text{ordre}}{f_{\text{éch}}} = c^{te}$$

So we have the relationship:

$$\boxed{\text{ordre} = c^{te} \cdot \frac{f_{\text{éch}}}{\Delta f}} \quad (1)$$

In this case, we have more:

$$\Delta f / f_c = 0,09 \quad (16\text{-channel case}) \quad \text{and} \quad \Delta f / f_c = 0,044 \quad (32\text{-channel case})$$

Let's consider the extreme case of the narrowest TNR filter in frequency, and therefore the widest time window.

In this case we have: $f_c = 4 \text{ kHz}$, and $f_{\text{éch}} = 64,1 \text{ kHz}$, so:

²⁴ This time-frequency correlation is equivalent to the well-known uncertainty principle in quantum mechanics.

²⁵ We recall that the order of a digital filter is the number of non-zero coefficients that define it.

16-channel case $f_{éch}/\Delta f = \left(f_{éch}/f_c\right) \cdot \left(f_c/\Delta f\right) = (64,1/4) \cdot (1/0,09) \approx 178$

32-channel case $f_{éch}/\Delta f = \left(f_{éch}/f_c\right) \cdot \left(f_c/\Delta f\right) = (64,1/4) \cdot (1/0,044) \approx 364$

In this case, by experiment $c^{te} \approx 1.4$ (or 1.3 TBC), and therefore the following window widths were chosen:

- in the case of 16 filters: 256.
- in the case of 32 filters: 512.

Therefore, 256 samples (16-filter case) and 512 samples (32-filter case) must be acquired to perform the filtering²⁶.

From formula (1) we can deduce that the order of a filter (thus the time taken to collect a block of samples) is determined by:

- the frequency band (because it determines $f_{éch}$: sampling theorem).
- the bandwidth of the filters²⁷.

In order to reduce the calculation time and to store fewer coefficients in the instrument's read-only memory (PROM), minimum order filters are sought. Thus, the number of coefficients used is a function of the number of channels in the band, decreasing as the frequency increases (see below).

4.6. Digital filtering

4.6.1. Position of the problem

The digital filtering is carried out by means of a bank of bandpass filters of the FIR²⁸ type, with a very narrow bandwidth and high dynamics. Details of the filter design are given in the appendix [MAN84, MAN94]. This is the same class of filters as those used for the RETE experiment of the TSS mission.

The advantage of using a filter bank rather than a fast Fourier transform is that the latter method would provide a set of uniformly spaced spectral points with the same spectral window of analysis for each, whereas with a filter bank it is possible to freely choose the center frequencies and bandwidths of each filter. Larger center frequency separations and wider bandwidths are thus possible at high frequencies, which represents an economy in terms of the number of coefficients to be stored. This is in line with the desired evolution of the

²⁶ As many samples are needed as the filter has coefficients, a digital filtering being a convolution operation of the type:

$$\sum_{i=0}^N \text{coefficient}(i) \cdot \text{échantillon}(N - i).$$

²⁷ The narrower the bandwidth, the longer the filter. Intuitively, this can be understood as follows: a filter with infinite bandwidth, i.e. a filter that has no effect, has only one coefficient of value 1. If we add constraints, we increase the complexity of the filter and we must therefore increase the number of coefficients to satisfy these constraints.

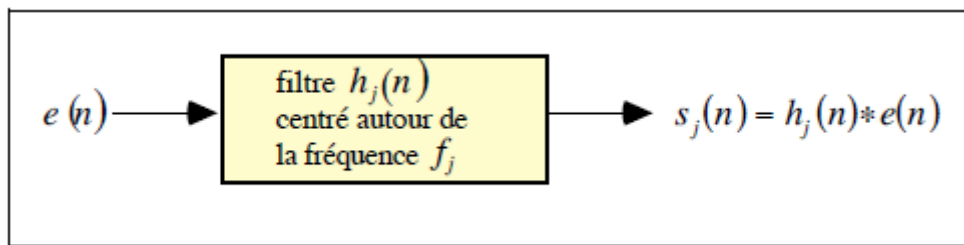
²⁸ Finite Impulse Response (FIR): Finite Impulse Response (FIR) filters - see Appendix.

spectral resolution: in particular, a good resolution around f_p is desired, the resolution at high frequency being less important. We choose $\delta f = c^{te} \cdot f$, where δf is the width of a filter and f its center frequency.

The aim here is not to calculate the spectrum of a single signal defined over the time interval $[-\infty, +\infty]$, but to follow the evolution of the spectrum of the signal collected by the antenna over time: a series of successive spectra is therefore calculated²⁹. For this purpose, the signal is analysed for a certain integration time, the value of which is controlled by the DPU, using 32 very narrow width filters. In the following, we will consider, for example, the case of spectra with 32 values and N blocks of 512 acquired samples.

4.6.2. Classic method

Let $e(n)$ be the digital signal received at the output of the C A/N, $h_j(n)$ the discrete impulse response of a bandpass filter, whose spectrum is centred on a centre frequency f_j , and $s(n)$ the signal at the output of this filter³⁰.



To obtain the instantaneous power³¹ of the output signal $s(n)$ in the spectral band centred around the centre frequency f_j , the square of the convolution product³² must be calculated. It is assumed that we start the filtering at time n_0 (with $n_0 \geq N_0 - 1$, to avoid having to take edge effects into account):

²⁹ It is therefore an analysis in time and frequency, which makes us think of a wavelet analysis of the signal (see appendices).

³⁰ As is customary in signal theory, we will omit the sampling step $\Delta t = 1/f_{ech}$ in the equations: the expressions $e(n)$, $s(n)$, $h(n)$ are respectively understood as $e(n\Delta t)$, $s(n\Delta t)$, $h(n\Delta t)$.

³¹ Let a continuous signal $x(t)$ be such that $|x(t)|^2$ is homogeneous to an instantaneous power, the energy contained in this signal in the interval $[t_1, t_2]$ is written

$$\int_{t_1}^{t_2} |x(t)|^2 dt$$

and the average power in this interval:

$$\frac{1}{t_2 - t_1} \int_{t_1}^{t_2} |x(t)|^2 dt$$

In the case of a discrete signal, $x(n)$, we can define in the same way the average power in an interval $[n_1, n_2]$:

$$\frac{1}{(n_2 - n_1)} \sum_{n=n_1}^{n_2} x(n)^2$$

³² The ADSP is well suited to convolution (multiplication-accumulation) calculations, the basis of digital filtering. More precisely, the ADSP is able, thanks to the MAC (Multiplier-ACcumulator), to perform the following sequence in a single instruction of 1 to 5 ns: total = total + $x_i \cdot y_i$; read from memory x_{i+1} ; read from memory y_{i+1} .

$$s_j^2(n) = (h_j * e)^2 = \left(\sum_{i=0}^{N_0-1} h_j(i) \cdot e(n-i) \right)^2 \quad \text{where } N_0 \text{ is the order of the filter. (1)}$$

The average power of the output signal is given by:

$$S_j = \frac{1}{N} \sum_{n=n_0}^{n_0+N-1} [s_j(n)]^2 = \frac{1}{N} \sum_{n=n_0}^{n_0+N-1} \left[\sum_{i=0}^{N_0-1} h_j(i) \cdot e[(n-i)] \right]^2 \quad (2)$$

where N is the number of sample blocks of the signal for this analysis (and also the total number of samples acquired, see figure). If N is too small, the result will be noisy. Otherwise, there is a smoothing effect (see § 4-7-2).

In theory, to calculate this average power for the 32 filters, i.e. to obtain a spectrum of 32 values, it would be necessary to proceed as follows (classical filtering by the principle of the sliding filter):

- acquisition of a first block of signal samples: $[e(n_0), \dots, e(n_0 + 512 - 1)]$
- calculation of $s_j^2(n_0)$ according to the formula (1), where j is an index designating the filter number:
 $1 \leq j \leq 32$. Accumulation of these values in memory.
- acquisition of a new sample $e(n_0 + 513)$.
- With $[e(n_0 + 1), \dots, e(n_0 + 513)]$, calculation of $s_j^2(n_0 + 1), 1 \leq j \leq 32$. Accumulation in memory.
- etc..
- acquisition of a new signal sample.
- calculation of $s_j^2(n_0 + N - 1), 1 \leq j \leq 32$. Accumulation in memory.
- average of $s_j^2(n_0 + 1), s_j^2(n_0 + 2), \dots, s_j^2(n_0 + N - 1)$, successively for $1 \leq j \leq 32$: we obtain S_j for $1 \leq j \leq 32$, i.e. a spectrum of 32 values.

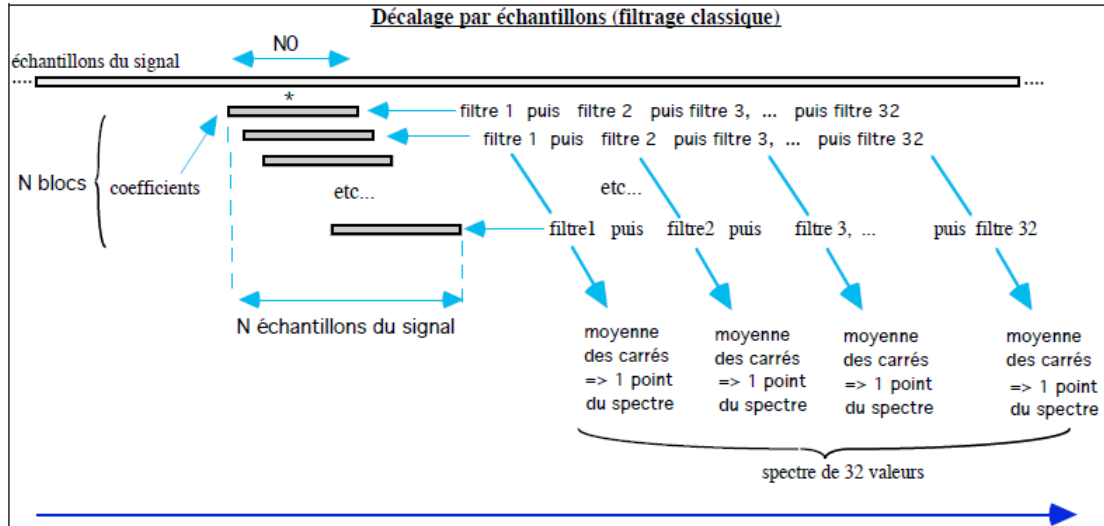


Fig. Offset per sample

4.6.3. Method used

The filtering on board the satellite must be performed in a near real time context. In the previous case, to perform $(N_0 = 512 \text{ multiplication-accumulations} + 1 \text{ average}) \times 32$ filters would require about 2 ms . The sampling rates are such that the samples are acquired much too fast to calculate 32 values of $s_j^2(i)$ before a new sample is acquired. For the A-band, for example, the frequency sampling rate is 64 kHz, so the acquisition time of a sample is $1/64 \cdot 10^{-3} \text{ s} = 0.0156 \text{ ms} \ll 2 \text{ ms}$. As a result, R. Manning proposed the following solution:

- acquisition of a first block of signal samples: $[e(n_0), \dots, e(n_0 + 512-1)]$
- calculation of $s_j^2(n_0)$ where j is an index designating the filter number: $1 \leq j \leq 32$. Accumulation of these values in memory.
- acquisition of a new block of samples $[e(n_0 + 512), \dots, e(n_0 + 2 \cdot 512-1)]$
- calculation of $s_j^2(n_0 + 1)$, $1 \leq j \leq 32$, Accumulation in memory.
- etc..
- calculation of $s_j^2(n_0 + N - 1)$, $1 \leq j \leq 32$, Accumulation in memory.
- average of $s_j^2(n_0 + 1), s_j^2(n_0 + 2), \dots, s_j^2(n_0 + N - 1)$ successively for $1 \leq j \leq 32$: we obtain S_j for
- $1 \leq j \leq 32$, i.e. a spectrum of 32 values.

This amounts to shifting the filter by blocks of samples, instead of shifting it at each sample as before. It is thus assumed that during the acquisition of a spectrum, this spectrum does not evolve much. In this way, the number of multiplications and additions of formula (2) is reduced by a factor N_0 by calculating only the quantity (in this equation N_0 depends on j):

$$S_j^2 = \frac{N_0}{N} \cdot \sum_{n=n_0}^{n_0 + N/N_0 - 1} s_j^2(n N_0) = \frac{N_0}{N} \cdot \sum_{n=n_0}^{n_0 + N/N_0 - 1} \left[\sum_{i=0}^{N_0-1} h_j(i) \cdot e[(nN_0 - i)] \right]^2 \quad (3)$$

N is the total number of acquired samples. N_0 is the order of the filter j . N/N_0 (1) is the number of blocks of acquired samples.

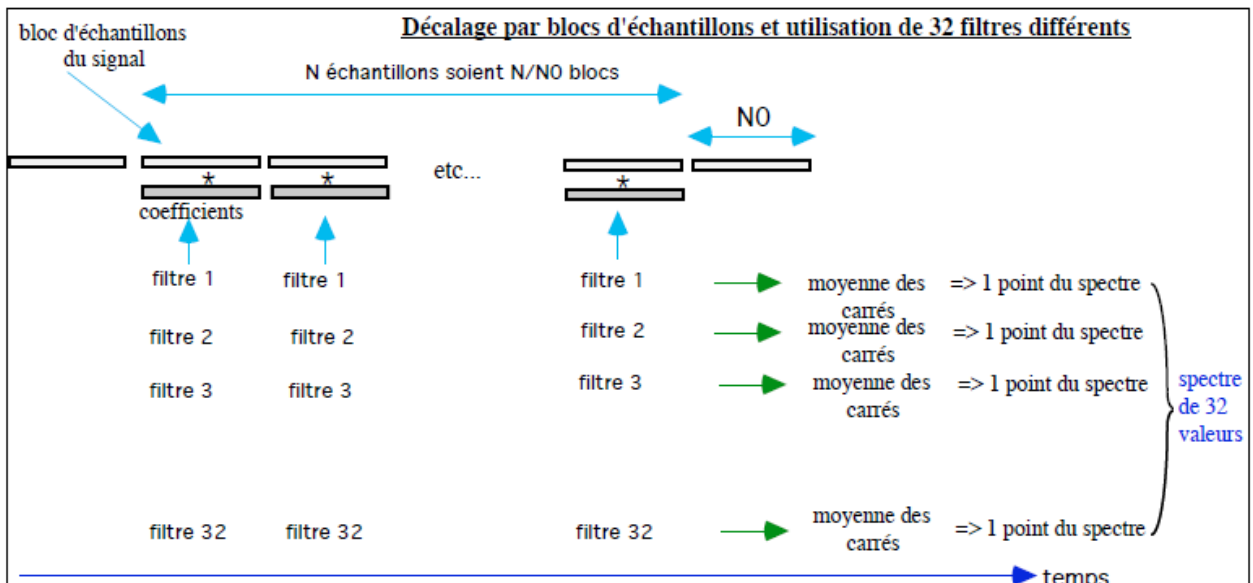


Fig. Shifting by blocks

Note:

This method has the following disadvantage: in the case of a purely sinusoidal wave, with a frequency equal to an exact sub-multiple of the sampling frequency (frequencies close to the harmonics of $f_{éch}/N_0$), one is led to systematically reconsider the same samples of the signal (beating phenomenon), and one thus has no statistical average. Here, the problem does not arise because we are studying a physical signal, whose energy is distributed over a certain range of frequencies

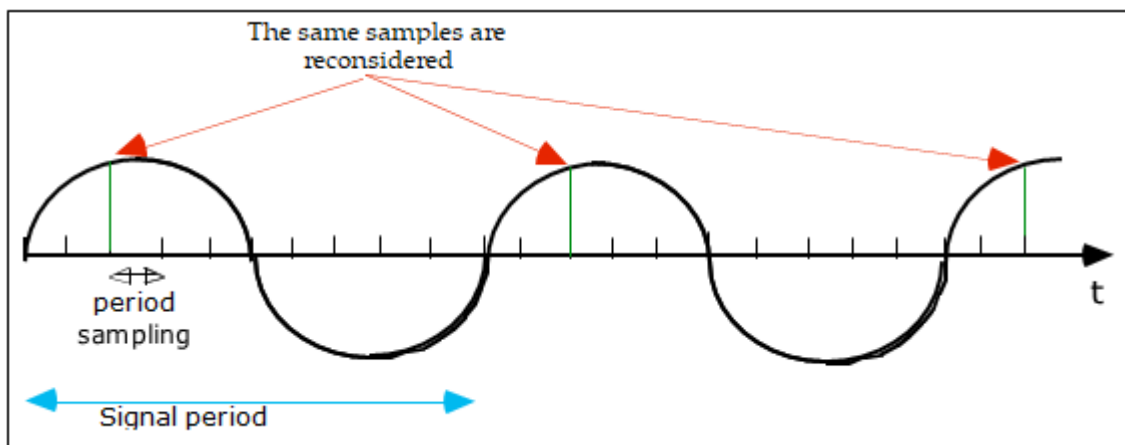


Fig. Case of a sinusoidal wave with a period multiple of the sampling period

4.6.4. Other reductions

The use of filters of similar shape but with a larger bandwidth, and therefore lower order, as the frequency increases (in the equations, this is reflected by the fact that N_0 depends on j) reduces the calculations by about 50% compared to the case of choosing filters of identical width in the same band.

Duration T ₀	Duration T ₁	Duration T ₂	Duration T ₃
1,472 s	$\frac{1,472}{2} = 0,736 \text{ s}$	$\frac{1,472}{4} = 0,368 \text{ s}$	$\frac{1,472}{8} = 0,184 \text{ s}$

These durations are exact multiples or sub-multiples of the duration of a minor frame (cf. § 2-3) which is 0.368 s. In 1.472 s, we have 4 minor frames ($4 \times 0.368 = 1.472$). The value 1.472 s corresponds approximately to half a period of rotation of the satellite.

By default, the integration time is:

- **1.472 seconds** in LBR (Low Bit Rate)
- **0.736 seconds** in HBR (High Bit Rate)

Let us recall the following data:

- The telemetry is composed of a succession of MFs. Each MF contains 250 mf. One mf corresponds to a duration of 0.368 seconds in LBR.
- The Waves experiment has a telemetry quota that corresponds to a packet of 431 words every 10 mf, or 3.38 seconds in LBR.
- In mode 2, for example, the DPU places 12 spectra (of 32 values each) in a packet. In effect, 12 spectra along with the AGC values and various headers used fit into a 431 word packet: $(32 + 1) \times 12 = 396 < 431$.
- It takes 1.472 seconds for the TNR instrument to make a spectrum of 32 values. It takes $12 \times 1.472 \text{ seconds} = 17.664 \text{ seconds}$ for the 12 spectra to be made.
- The DPU has to wait for $5 \times (10 \text{ mf})$, i.e. $5 \times 3.68 = 18.4 \text{ seconds}$, to fill a TNR packet. Since an MF contains 250 mf, or $250 / 10 = 25$ packets, it will be possible to place 4 TNR packets in an MF, out of the 25 it contains. The other packets are obviously allocated to the other experiments (RAD1, RAD2, TDS, FFT).

Reducing the integration time of a spectrum would place more than 4 TNR packets in a MF and encroach on the telemetry allocation of other experiments.

- By repeating the same calculation with a TNR spectrum integration time of 0.736 seconds and a telemetry HBR rate (one MF lasts 46 seconds and one mf lasts 0.184 seconds), it can be verified that 4 TNR packets can still be placed in one MF. The TNR telemetry allocation rate remains the same. The result is that there are twice as many TNR spectra in HBR: there are as many TNR spectra in HBR as in LBR in an MF, but the MF lasts half as long in HBR.

The inherent ability of the TNR instrument to achieve low integration times³⁷, down to 0.184 s, is limited by the nominal telemetry rate allocated to it. This possibility implies the use of part of the telemetry rate nominally allocated to another instrument, as part of the rate allocated to the Waves experiment. This option is nevertheless used from time to time during the mission. Note that the high telemetry rate for the first two years allows the use of an integration time of 0.736 s.

³⁷ As already indicated, this possibility of fast analysis and therefore high temporal resolution allows the study of micro fluctuations of the local electron density.

This rapid integration is one of the original features of the Waves experiment, as the time resolutions obtained for the latest DESPA plasma missions are much lower.

4.7.2. Consideration of the integration period

In order to ensure that the calculation time of a spectrum by the TNR instrument corresponds to the integration time ordered by the DPU, the number N of series accumulated in memory is adjusted accordingly³⁸. In practice, it is ensured that the complete processing is completed sufficiently in advance of the next acquisition: the sum of the acquisition time (a few ms), the calculation time of the 16 or 32 filters (1 to 10 ms) and the transfer time to the DPU (of the order of 70 ms)³⁹ must be less than or equal to the integration time controlled by the DPU:

$$N \cdot (\Delta t_{\text{acquisition}} + \Delta t_{\text{filtrage}}) + \Delta t_{\text{transfert}} \leq \frac{1472}{n} \text{ ms}$$

with $n = 1, 2, 3, 4$

In this expression, we do not include the other times (8-bit compression of the data, calculation of the NN: additional calculations, normalization, propagation: 0.47 ms, ...), which are negligible.

The table below shows the number of blocks by which the results are averaged, depending on the TNR mode and the frequency band in force.

N.B. The AGC and numerical values of the spectrum are averaged by these same values.

	Mode 2,3 Number of blocks of 512 samples collected				Mode 0.1 Number of blocks of 256 samples collected				Mode 4 Number of blocks of 256 samples collected			
	T0	T1	T2	T3	T0	T1	T2	T3	T0	T1	T2	T3
Band A	144	72	36	17	296	148	74	37	272	135	67	33
Band B	258	128	63	31	545	272	135	67	465	232	116	57
Band C	427	213	106	52	927	463	231	115	730	364	182	90
Band D	633	316	157	78	1450	725	362	181	1007	503	251	125
Band E	844	422	211	105	1994	997	498	249	1265	632	316	157

The number of blocks to be processed varies from 17 to 1994. It can be seen that this number increases for the highest frequency bands (because the sampling speed is then high), and obviously when the integration time increases.

In the case of the A-band, for example, the sampling frequency is 64 kHz. The acquisition time for a block of 256 samples is therefore $256/64000=4$ ms. Once acquired, this block is processed, which corresponds to a certain time. Therefore, for an analysis period to last, for example, 1.472s, the TNR must repeat the sample/process sequence many times, accumulating results as it goes. In either mode 0 or 1, the TNR will repeat the sample/process sequence 296 times in 1.472 s.

Note: The greater the number of averages N , the more the random fluctuations decrease. Beyond a hundred

³⁸ The other instruction sequences do not offer this flexibility because they correspond to constant microprocessor instruction times.

³⁹ This transfer time of data from the TNR to the DPU is unknown and variable. It is therefore increased.

averages, these fluctuations become smaller than the digitization step. For the first frequency bands, in particular A and B, and for low integration times, the values of N become low. However, experience has shown that the signal-to-noise ratio remains acceptable under these conditions.

4.7.3. Data compression

In order not to clutter the telemetry system, the spectra values (initially coded on 32 bits - TBC) calculated on board are compressed according to a quasi-logarithmic scale, into 8-bit words. These 8-bit words are transmitted to the DPU and then to the telemetry.

This compression is carried out in the following way: by traversing, starting from the left, the binary sequence of the 32-bit word to be compressed, one locates the position, noted E (for Exponent), of the first non-zero bit. The 32-bit word can then be written:

$$N = 2^E + \alpha_1 2^{E-1} + \alpha_2 2^{E-2} + \alpha_3 2^{E-3} + \dots + \alpha_E 2^0$$

with α_i taking the values 0 or 1.

Or else:

$$N = 2^{E-3} (2^3 + \alpha_1 2^2 + \alpha_2 2^1 + \alpha_3 2^0) + \text{neglected terms}$$

That is:

$$N \approx 2^{(E-3)} (8 + M)$$

with:

$$M = \alpha_1 2^2 + \alpha_2 2^1 + \alpha_3 2^0$$

The information contained in this approximation of N is thus reduced to the knowledge of E and M (i.e. α_1 , α_2 and α_3). Since E can be between 0 and 31, 5 bits are needed to encode it: they will occupy the 5 MSB⁴⁰ of the final 8-bit word. There are still 3 bits available to code the coefficients α_1 , α_2 and α_3 : they will occupy the 3 LSB of the final 8-bit word (mantissa M).

Example :

n° de bit	31	30	29	28	27	26	25	24	-----	0
valeur	0	0	0	0	1	1	0	1	-----	---
									termes négligés	
									--	

E=27 $\alpha_1=1$ $\alpha_2=0$ $\alpha_3=1$

Putting $2^{(E-3)}$ as a factor, we get:

⁴⁰ MSB: Most Significant Bit and LSB: Least Significant Bit.

$$N = 2^{E-3} (2^3 + \alpha_1 2^2 + \alpha_2 2^1 + \alpha_3 2^0)$$

The term $\alpha_1 2^2 + \alpha_2 2^1 + \alpha_3 2^0$ being called the mantissa, noted M, we can write:

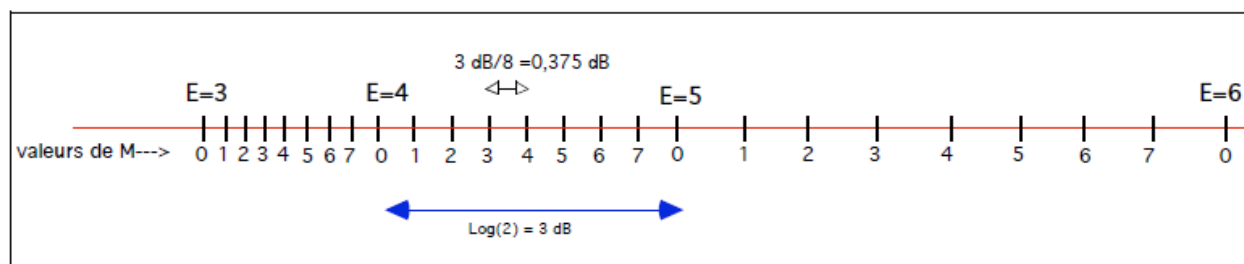
$$N = 2^{(E-3)} (8+M)$$

This formula is used to decompress the 8-bit telemetry words.

We can see that between two values of E, the transfer rule is linear (in power). For E ranging for example from 3 to 5 (M taking values between 0 and 7), the possible values of N are: 8, 9, 10, 11, 12, 13, 14, 15, 16, 18, 20, 22, 24, 26, 28, 30, 32, 36, 40, 44, 48, 52, 56, 60. Each time E increases by one, the term 2^{E-3} is multiplied by 2, resulting in a difference of

$$10 \log \left(\frac{2^{E+1-3} (8+0)}{2^{E-3} (8+0)} \right) = 3 \text{ dB}$$

However, for each value of E, there are 8 possible values of M (3-bit coding of M): the representation of a value by means of this compression technique can therefore only be given to the nearest $3 \text{ dB} / 8 = 0.375 \text{ dB}$.



4.7.4. Communication TNR-DPU

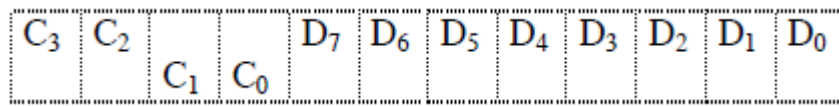
Between two acquisitions, the TNR is waiting for a command from the DPU, which occurs in the form of a software interrupt. This interrupt, if validated, points to a given sequence of instructions in the ADSP code. The command is then processed and any results are transmitted to the DPU. The TNR then resets itself to the position of waiting for a software interrupt from the DPU.

In the case of an analysis command (spectrum calculation, f_p calculation), which is the basic command, the DPU commands the TNR to position itself on a given band and waits for the response. The DPU must send a command for each frequency band it wants the TNR to position itself on. Thus, when the DPU is in ABCDE scan mode, the following commands are transmitted from the DPU to the TNR:

...
 process band A process band B process band C process band D process band E process band A
 process band B process band C process band D process band E

...
 Commands from the DPU are coded on 12 bits: 4 bits (letter C below) to designate the type of command and 8

specific bits (letter D below) for the command parameters:



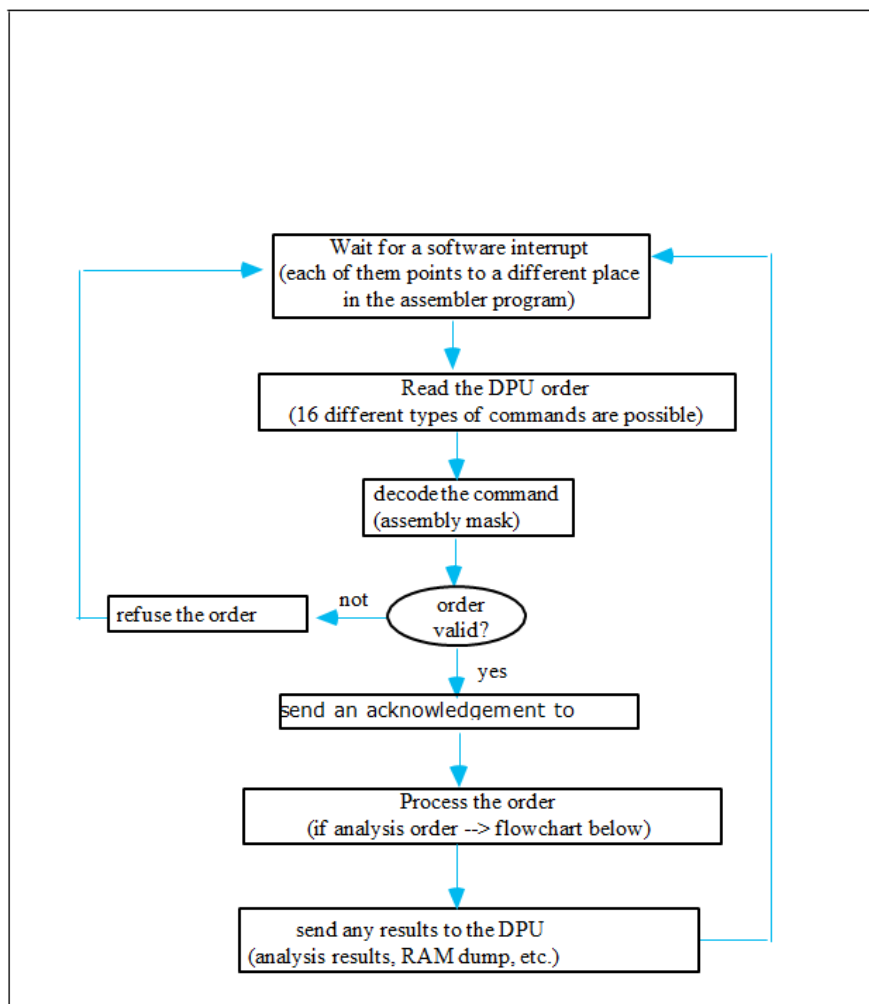
See the header of the TNR management program written by Liam Friel for details of this coding in the general case. In the case of an analysis command, the 4 left bits (MSB), which are used to code the command sent, are zero, and the coding is as follows:

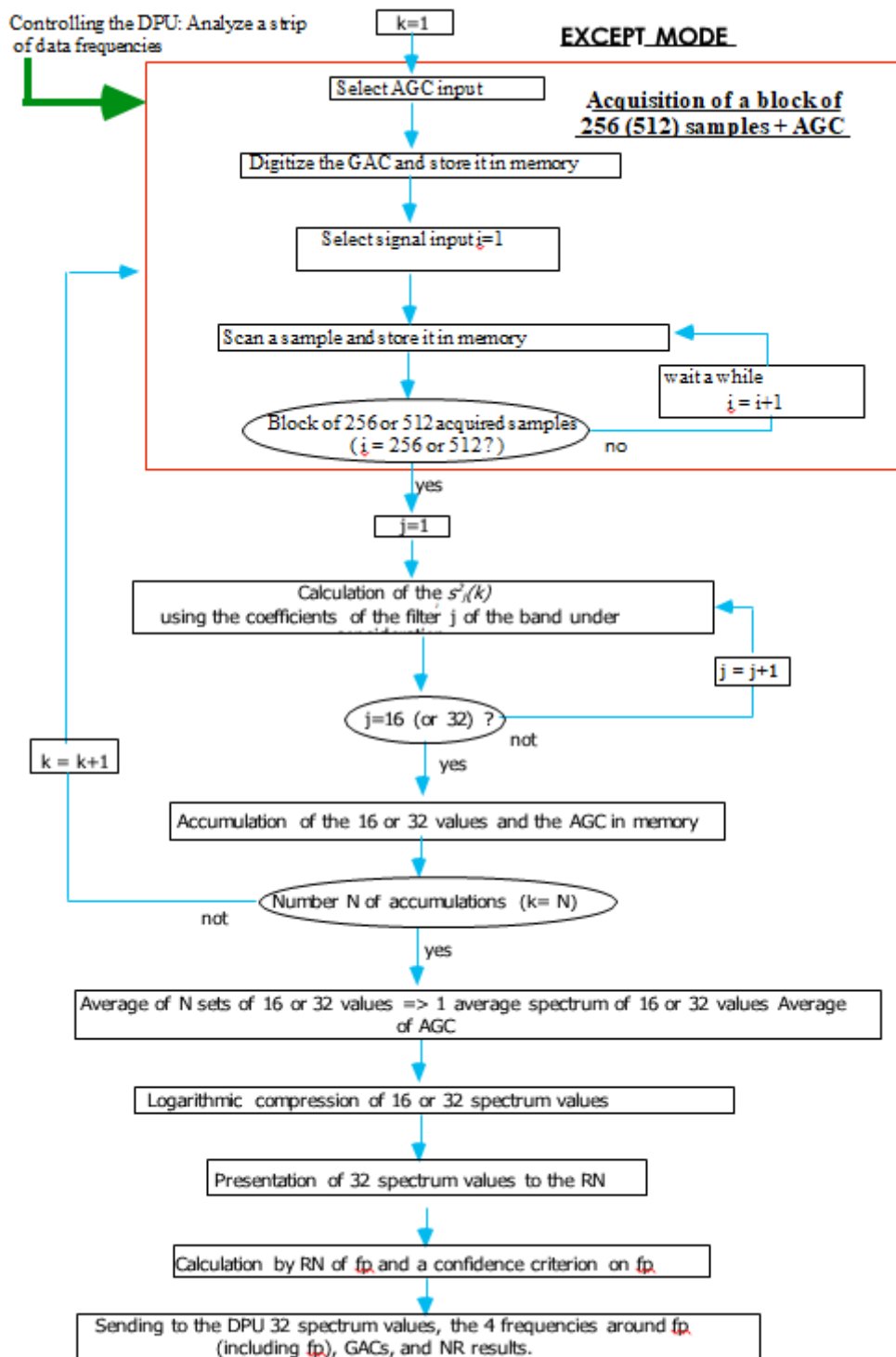


I₁ and I₀ : code the integration time (00: 1.472 s, 01: 0.736 s, 10: 0.368 s, 11: 0.184 s).

M₂, M₁ and M₀: code the TNR mode: 0 to 4.

B₂ B₁ and B₀: code the band to be analyzed: A, B, C, D, E.





4.8. Learning process

4.8.1. Principle

The position of f_p varies in time and space⁴¹: detectable from 4 kHz, it can reach 80 kHz and more. It is therefore necessary to be able to follow it over time. To do this, we use a supervised Pattern Recognition (PR) method⁴²: in this case, a Formal Neural Network (FN), trained to identify the position of f_p (see appendix).

The principle of learning⁴³ consists in using the RN to classify the successive spectra⁴⁴ of the signal: the spectra of the learning base are successively presented at the input of the RN with, for each, the associated f_p value as a target, at the output of the RN. The synaptic coefficients resulting from this learning are stored in the PROM memory of the TNR instrument. This RN is thus in principle able, from a spectrum measured in flight, to determine the associated f_p value⁴⁵.

The learning is done on the ground before launch, from spectra collected in the ULYSSE/URAP experiment, adapted to the characteristics of the TNR receiver. A learning is also implemented during the mission from spectra actually calculated on board: this allows to download new synaptic coefficients.

4.8.2. Pre-treatment

4.8.2.1. Increase in dynamics

Before presenting the spectrum values to the NN, their dynamic range is increased by re-normalizing them from 0 to 255, i.e., if we call x_i the spectrum value of channel ii after compression⁴⁶, and y_i the same value after increasing the dynamic range:

$$\begin{aligned} y_i &= 255 \frac{x_i - x_{\min}}{x_{\max} - x_{\min}} & \text{si } x_{\max} - x_{\min} \geq 32 \\ y_i &= 8 \cdot (x_i - x_{\min}) & \text{si } x_{\max} - x_{\min} < 32 \end{aligned}$$

⁴¹ Remember: the plasma frequency is related to the local electron density N_e by the relationship

$$F_p(\text{kHz}) = 9,1 \sqrt{N_e(\text{cm}^{-3})}$$

The electron density N_e is a function which decreases roughly in R^{-2} , R being the distance to the sun.

⁴² Cf. annexes.

⁴³ The specification (structure definition, learning) and the validation (tests, performances) of the NN of the TNR instrument were the subject of Philippe Richaume's thesis [RIC94, RIC96], to which we refer for more details.

⁴⁴ In data analysis, we usually differentiate between the notions of "classification" (associated with automatic classification) and "classification" (see appendices).

⁴⁵ In particular, this requires that the training file used be sufficiently representative. This problem is a constant in RDF.

⁴⁶ The compression of the spectrum values is performed before they are read by the NN. The learning process is therefore based on 8-bit coded values (E, M), and not on the real values. The possibility of performing mathematical operations on compressed values is due to the fact that the logarithmic compression used respects approximately the size of the number to be compressed. However, this process is still open to question.

The second case ($x_{max} - x_{min} < 32$, the value 32 is chosen arbitrarily low) aims at avoiding a sudden increase of the dynamic range which would risk amplifying only noise, when the spectral signature is of low amplitude.

This dynamics transformation affects the spectrum quite strongly but should have little influence on the detection of f_p (TBC). The influence on parameters other than f_p remains to be validated.

The first equation implies $y_{max} - y_{min} = 255$, the second $y_{max} - y_{min} = 8 \cdot (x_{max} - x_{min})$. The curve representing the dynamics obtained after rescaling $y_{max} - y_{min}$, as a function of the dynamics before rescaling $x_{max} - x_{min}$ is therefore the following:

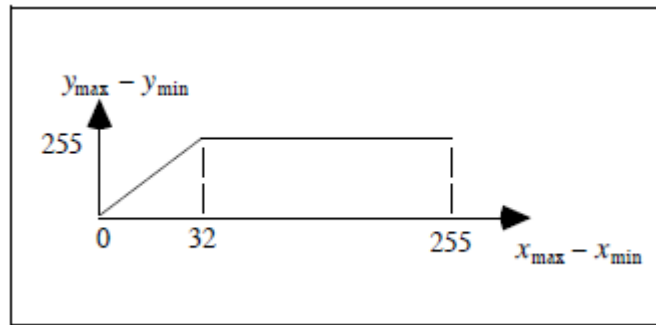


Fig. transformation of the dynamics

4.8.2.2. Standardized treatment of 16 or 32 entry cases

In order to simplify the on-board software, a single NN with 32 inputs (actually 35, see above) is used, even to process a spectrum of 16 values. In the latter case, we proceed as follows: if we call e_i ($i = 0, \dots, 15$) the 16 values of the spectrum computed by filtering, we apply to the 32 inputs of the NN the following quantities - simple average:

NN entry number	0	1	2	3	29	30	31
Value	e_0	$e_0+e_1/2$	e_1	$e_1+e_2/2$	etc...	$e_{14}+e_{15}/2$	e_{15}	e_{15}

In mode 4, only the 16 TNRA (AC) spectrum values are presented to the NN, as otherwise it would be presented with data of a hybrid nature: 16 values from TNRA and 16 values from TNRB.

It can be seen that this procedure leads to repeating the last e_{15} value.

4.8.3. NN Characteristics and Learning

The choice was made for a NN "Multi-Layer Perceptron" (MLP)⁴⁷. The number of layers chosen is three.

- 35 input layer neurons: 32 spectrum values, the AGC, the band number (coded 0 for band A, 1 for band B, etc...), and the bias (which is systematically 255).

- 12 neurons in the hidden layer, plus the bias (255).

⁴⁷ This is one of the most common NN structures.

- 32 neurons in the output layer: each of the outputs i ($0 < i < 31$) of NN⁴⁸ can take a value $v(i)$ between 0 and 255.

It is therefore an MLP 34-12-32 for short.

During training, for a given spectrum presented at the input of the NN, the NN output corresponding to the position of f_p is assigned the value 255, while the other outputs are assigned the value 0. In the test phase, the position j associated with the highest of the output values is designated as the plasma frequency ($j = \hat{f}_p$) by the NN. The value $v(f_p)$ will be considered as the confidence index of the result provided by the NN. This is because, this value will in principle be higher the better the NN has recognized f_p . When a spectrum is not clearly assigned by the NN to one of the classes (a channel), it is assigned to a class called "rejection" class (a rejection "threshold" must be defined a priori).

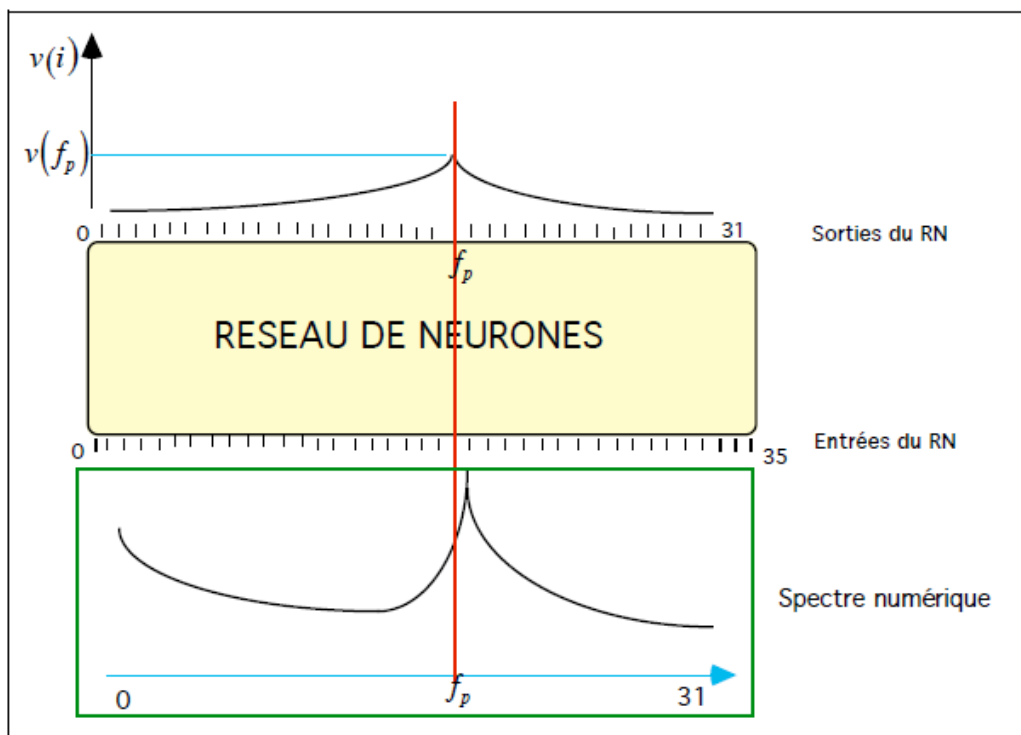


Fig. Operation of the Neural Network (NN or RN) in test phase.

The training of the spectra base is performed by the now classical gradient back-propagation technique. The transfer function of the formal neurons is a sigmoid⁴⁹. Its values are tabulated rather than calculated on board. Only one sigmoid arch is stored in memory: by central symmetry, the other arch can be reconstructed. It has the following appearance:

⁴⁸ The coding of the outputs of a NN can be chosen by the user: binary outputs, taking continuous values, etc... Various comparative tests have been carried out [RIC96].

⁴⁹ There are 256 resolution points on the ordinate. If the abscissa points (potential values) were too widely spaced, some of the ordinate points would never be reached, especially near the inflection point, where the slope of the sigmoid is high. The number of points required on the x-axis to reach all the points on the y-axis was calculated. On the other hand, when the calculated abscissa is greater than 8192, $f(x)$ is forced to 255, when it is less than -8192, $f(x)$ is forced to 0.

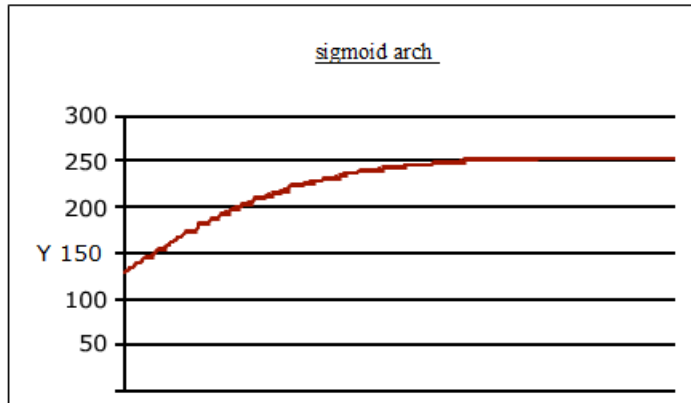


Fig. Sigmoid arch - activation function of a formal neuron

It is possible to modify the weights of the NN and the number of neurons per layer⁵⁰ after launch. This replacement is done by downloading a more or less important part of the software or "patch"⁵¹. During ground learning, the determination of the synaptic coefficients of the NN is carried out using of a powerful computer⁵². These are then adapted to take into account the memory representation of the ADSP (*16 bits possibly signed*).

The rates of well-classified observations, within one channel, obtained for this NN are [RIC96]:

learning file ⁵³ of well-classified observations	95,4%
test file containing spectra with a plasma line fairly well differentiated	96,6%
test file containing highly disturbed spectra	83,4%

N.B. Routine NN validation consists of verifying that the results provided by the NN corroborate those obtained by numerical fitting, using a test file containing a large number of spectra. Such a possibility is under study.

4.8.4. Remarks

4.8.4.1. Quality of the learning base

⁵⁰ The number of layers has been fixed at 3. It can only be modified by reorganizing the ADSP program, whereas the number of neurons per layer is only a parameter of the program and can therefore be modified more easily.

⁵¹ This is an explicit image for an English speaker: a "patch" is a piece of cloth intended to cover a tear in an item of clothing. At launch, the PROMs contain the ADSP program and its parameters (filter coefficients, NN, sampling frequencies, etc.). They are said to be "burned", before launching. At RESET, this information is loaded in the RAM. From this moment on, the ADSP executes the program that is in this RAM. In case of a "patch", the ADSP receives from the DPU a new set (TNR program + parameters): the microprocessor writes them in the RAM, replacing the previous (program + parameters). The DPU works differently: the NS microprocessor talks to the PROM - which has a much longer access time - and not the RAM. More precisely, the RAM contains a list of addresses, each pointing to the beginning of a task contained in the PROM. For execution, the microprocessor scans this address table. However, this strategy lacks flexibility, as it is only possible to download new sequences into the DPU RAM. It is therefore very difficult to patch the DPU.

⁵² CONVEX machine: 32-bit floating point calculations.

⁵³ This is the apparent rate, see Annex 4.

The detection of f_p can be made difficult by various factors. In particular, the NN may no longer be able to track the position of f_p , due to various types of emission that change the shape of the collected spectrum, as well as the various irregularities that typically affect it. Type III bursts are a fairly common case. AKR radiation is also a nuisance above 150-200 kHz. It should be noted that the plasma frequency is a characteristic cut-off frequency of the medium for all these potential disturbances. The problem of what to do when the spectrum contains other strong emissions, which prevent automatic tracking of the plasma line, is not resolved⁵⁴.

The performance of the NN is, as for any RDF system, a function of the sharpness of the shapes to be recognized. Here, in order to be easily recognizable, the spectra must in particular present a well differentiated steep front at f_p . The fact that the DPU constructs a histogram of the NN results over a certain time period (see above) limits the effect of NN recognition errors.

4.8.4.2. Limitation of telemetry allowance

Selecting scientific parameters in flight by means of an automated system, rather than on the ground by more conventional methods, poses the problem of arbitrary detection and the risk of new or unexpected events being missed. That said, it is worth remembering that data loss due to telemetry limitations is an inevitable phenomenon⁵⁵.

The use of an NN for the selection of scientific parameters in flight (here, the case of the "fast" mode) can be compared, from the point of view of the goal to be reached, to that of data compression implemented in the framework of other space missions (Cassini/RPWS at DESPA): these two techniques make it possible, among other things, to circumvent the problem of the limitation of the telemetry flow.

4.8.4.3. Evolution of NN structure

The possibility of downloading a new sequence of ADSP instructions ("patch") during the mission, makes it possible to envisage modifications to the NN, taking into account the memory space in the TNR, and of course, the scientific opportunity (regions overflowed by the probe, results obtained, ...). These modifications must of course be tested beforehand on the Engineering Model.

As the position of the plasma line evolves in a non-random way in the course of time, an improvement of this model can be envisaged, by taking into account the successive results of the NN: for example, by adding n inputs to the NN, these inputs receiving for the calculation at time n the outputs of the NN at times $n-1$, $n-2$, ..., $n-p$, the number p remaining to be defined. The realization of such a structure is possible by means of a looped NN with shift register (recurrent network). Other structure choices are possible⁵⁶.

⁵⁴ This poses a well-known problem in RDF: if the machine allows a quantification inaccessible to humans without tools, it shows limits in recognizing complex or noisy signals, even at the cost of sophisticated algorithms. If one wishes to refine the recognition process, i.e. to reduce the error or rejection rate, other discriminating criteria must be introduced, for example by appealing to semantic considerations. However, this approach is not systematically fruitful and, in any case, the resulting algorithmic complexity is hardly compatible today with the limitations of on-board spatial instrumentation, particularly in terms of memory and processing speed.

⁵⁵ The possibility of unsupervised learning in flight, i.e. the automatic detection and transmission of similar patterns, is a possibility that has been little or not explored. Note that in the same Waves experiment, the TDS module (Waves 2) contains a program that selects interesting events from events assumed to be associated with noise, but based on an algorithm defined on the ground.

⁵⁶ Recurrent networks, Time Delay Neural Networks cf. [RIC95].

Because of a certain temporal correlation in the signal describing the evolution of the plasma frequency, the history of f_p provides an indication that allows its prediction to be improved. In the case of a signal assumed to be stationary of the second order, the mathematical concept that accounts for this phenomenon is autocorrelation⁵⁷: $c(\tau) = E[x(t)x(t-\tau)]$. Different options are possible within a structure neuronal [RIC96].

4.8.4.4. Detection of the line at $2f_p$

The analysis of the first results of the Waves experiment has shown that electromagnetic waves at the double harmonic frequency of $f_p : 2f_p$, whose source is probably located near and upstream of the Earth shock, are observed with a fairly good precision and more often than expected. These waves are associated with energetic electrons moving along the magnetic field lines connected to the earth shock. In fact, the frequency is harmonic of the plasma frequency of the emission site, upstream of the earth shock. There is thus a slight time shift perceptible in the dynamic spectra. Its influence has not been sufficiently taken into account in the spectra of the ULYSSE/URAP experiment used to train the NN. In particular, the line at $2f_p$ can be confused with the line at f_p , which is not without problems.

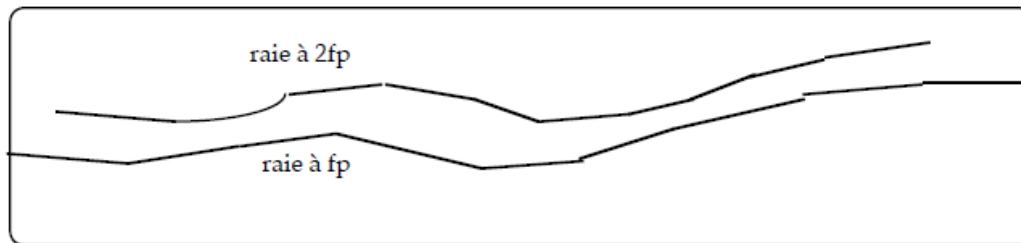


Fig. example of a spectrum with line at f_p and $2f_p$ (dynamic spectrum: summary plots)

(to be corrected: actual values)

To avoid this problem, on the ground, a training can be performed from spectra measured by the TNR instrument including all 48 or 96 channels, where the $2f_p$ line is in principle present.

Note: The electron density determined by the NN of the TNR instrument is available as a file in CDF format at 3 minute resolution.

4.9. Estimation of the parameters f_p , T_c , α , τ

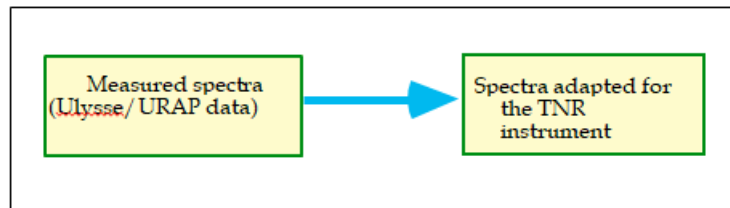
4.9.1. Digital adjustment

Pre-launch training of the NN requires a set of spectra similar to the spectra acquired by the instrument during the mission. These spectra are presented as input to the NN and the f_p value associated with each of the spectra is the NN target. To do this, we use the data from the ULYSSE/URAP experiment, adapting them to the particularities of the TNR receiver: **decalibration** of the data to the physical values at the input of the URAP⁵⁸ RAR receivers, spline interpolation of the missing values at the TNR frequencies, simulation of the AGC, among

⁵⁷ The Wiener Kintchine theorem states that the autocorrelation of the signal is the Fourier transform of the power spectral density.

⁵⁸ The ISEE3/ICE database was used in 1989 to validate the NN approach.

others. These transformations, made necessary by the instrumental differences between the WIND and ULYSSE receivers, are nevertheless sources of error and the reliability of the training file is only partial. However, such a file has the great advantage of providing a series of spectra over a long period (one year). Only the collection of spectra actually acquired during the mission by the TNR receiver can validate the training, i.e. the synaptic coefficients [RIC96].



For each of these experimental spectra, the associated value of f_p can be determined: a numerical fit determines, from an experimental spectrum and the theoretical expression of the spectrum, the four parameters f_p , T_c , $N_c/N_h = \alpha$, T_c/T_h . For the training of the NN, only f_p is retained⁵⁹ in the first instance. In some difficult cases, where the fit is erroneous, the value of f_p is determined visually (about 1/3 of the cases). On the other hand, the ratio between the number of parameters to be fitted and the number of points on the curve must be as high as possible. In this case, this number is limited to 40 in the case of URAP data; in practice, it is lower.

For the case of WIND data, about 40 000 to 80 000 sufficiently well-fitted spectra are retained: 41 000 for the B-band, 78 000 for the B-band, 47 000 for the C' band [12 - 48 kHz]: as the "ULYSSE low" frequencies are limited to 48.5 kHz, a pseudo C' learning band has been built up, to approximate the frequency range of the C-band [16 kHz - 64 kHz] of the TNR⁶⁰

We therefore have a certain number of $V^2_{mesuré}(f)$, f being the reception frequency. On the other hand, the physical modelling of the problem leads to the theoretical expression of the quasi-thermal noise spectrum⁶¹ $V^2_{théorique}(f)$, which is a function of the 4 parameters f_p , T_c , α , τ . The fitting⁶² of an experimental spectrum to the theoretical spectrum is performed by means of the classical technique of Levenberg and Marquardt⁶³, which consists in a minimization of the following cost function, derived from χ^2 .



⁵⁹ The electronic temperature is also a possible target of the NN, but it was not taken into account in the ground learning phase. Since it is a cut-off frequency, which results in a generally fairly steep slope in the spectrum, the value of f_p is undoubtedly the easiest of the four parameters to detect, even visually. It does not require precise calibration. It is also the one of greatest scientific interest (density measurement), which justifies the primary interest given to its determination by the NN.

⁶⁰ An initial set of about 144,000 Ulysses spectra (326 useful days between 4/11/90 and 30/09/91, low frequencies, .SPU file), of which about 130,000 are fitted. During this period, the probe was in the ecliptic plane between Jupiter and the Earth. The constitution of the learning base is carried out by Claude Perche from whom we will get more precise information.

⁶¹ This modelling is particularly complex, see the appendices [MEY80].

⁶² A simplified expert system written by S. Hoang is used to determine the value of f_p (detection of the cut-off point, verification of the spectrum decay in f^3 beyond, in the high frequency part). During the numerical adjustment, it provides an initialization value for f_p .

⁶³ Cf. annexes.

Find the values of the parameters f_p , T_c , α , τ , and that make the following cost function minimal:

$$C(f_p, T_c, \alpha, \tau) = \sum_{i=i_1}^{i_2} \left(V_{théorique}^2(f_i, f_p, T_c, \alpha, \tau) - V_{mesure}^2(f_i) \right)^2 \quad \text{avec } 1 \leq i_1, \quad i_2 \leq 64$$

The above summation covers a portion⁶⁴ of the 64 frequencies of the ULYSSE/URAP low frequency receiver⁶⁵: 1.25 kHz to 48.5 kHz, in steps of 0.75 kHz. The interval $[i_1, i_2]$ is chosen from an expert performed visually (detection of the upstream and downstream trough). The minimization program must know the values of $V_{théorique}^2$ and its derivative for a certain value of f , f_p , T_c , α , τ . The variable is f and f_p , T_c , α , τ are the parameters to be adjusted.

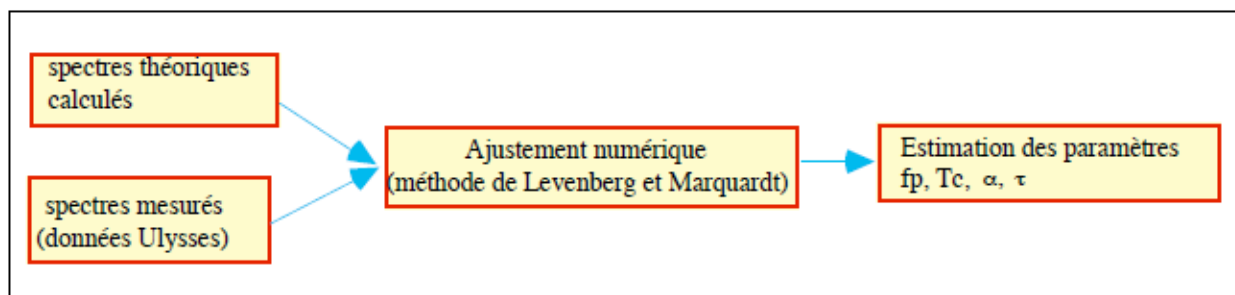


Fig. Block diagram of the parameter calculation

Note that in practice, the adjustment of QTN spectra is not always an easy operation to perform. This is due in particular to the possible presence of type III bursts (the program may mistakenly fit such a signal instead of the plasma line), and to the various noises that usually affect it. This limits the degree of automaticity of the processing of the spectra base, whether it is a question of adjustments of the training base or of the spectra measured in flight.

4.9.2. Cubic interpolation

Due to the complexity of its mathematical expression, the numerical calculation of $V_{theoretical}^2(f, f_p, T_c, \alpha, \tau)$, is only directly conceivable for a limited number of quadruplets f_p, T_c, α, τ . These define a "grid" in dimension 4. The number of values for which one calculates directly is the following⁶⁶:

$$(65 \text{ values of } f_p) \times (13 \text{ values of } T_c) \times (4 \text{ values of } \alpha) \times (4 \text{ values of } \tau) \times (40 \text{ values of } f/f_p).$$

Let: $(65 \cdot 13 \cdot 4 \cdot 4) \cdot 40 = (13\,520 \text{ spectra}) \times (40 \text{ values of } f/f_p) = 540\,800$ "nodes" in the grid.

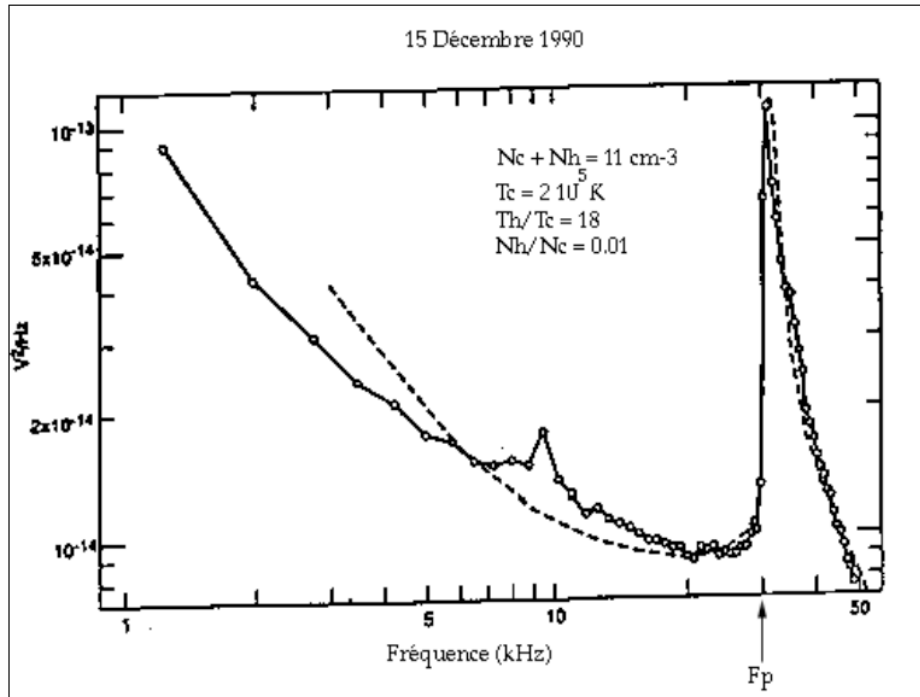
The values of $V_{theoretical}^2(f, f_p, T_c, \alpha, \tau)$ will thus be obtained by interpolation between the "nodes" of the grid.

⁶⁴ The thermal noise model does not currently take into account either the impact noise or the drift velocity of the plasma with respect to the antenna: it is therefore preferable to select only a part of the 64 points of a Ulysses/URAP spectrum. We therefore choose a limited interval around f_p .

⁶⁵ C. Perche notes that f_p is very poorly observed in the high Ulysses frequency range from 52 to 940 kHz; the corresponding spectra are therefore not used. This is less true when the probe is near Jupiter.

⁶⁶ Theoretical spectra base was formed for $0.1 < f/f_p < 10$, with 20 points on either side of f_p , logarithmically spaced.

The method (called spline-cubic method) used is the cubic interpolation -polynomials of the 3rd degree by pieces-multidimensional, of dimension 4.



Adjustment of the thermal noise spectrum. Position of f_p .

4.10. Ground data transmission

4.10.1. Transmitted data from TNR to DPU

It is recalled that there are 5 different modes of operation of the TNR instrument:

Mode of the TNR	Receiver(s) read	Number of frequencies per spectrum
0	TNRA	16
1	TNRB	16
2	TNRA	32
3	TNRB	32
4	TNRA (16 freq.) and TNRB (16 freq.)	16

The TNR systematically transmits 32 values to the DPU (in modes 0 and 1, it therefore transmits 16 zero

values in addition to the TNRA or B data, which the DPU does not transmit to the telemetry).

The data transmitted by the TNR to the DPU at the end of each measurement period are systematically as follows (note $v(f)$ the spectrum value at frequency f):

- 2 NN results: f_p (value from 0 to 31), confidence criterion of f_p .
- 1 spare word (zero byte).
- 2 words from AGC⁶⁷.
- 4 frequencies⁶⁸ around f_p (f_p included): $v(f_p - 2)$, $v(f_p)$, $v(f_p + 1)$, $v(f_p + 5)$.
- 1 spare word (zero byte).
- 32 values ($v(f)$, or $v(f)$ and zero values).

That is to say a total of 42 words of 8 bits (including 2 separation words).

The purpose of the DPU fast mode is to make the best use of the allocated telemetry rate. In this mode, not all data is transmitted, but only 4 frequencies around f_p (including f_p). These 4 values have been chosen so as to allow, in principle, an approximate reconstruction of the spectrum on the ground, from only 4 of its points⁶⁹.

The DPU fast mode was implemented in August 1996. It requires a higher throughput than the nominal throughput of the TNR instrument and therefore a different distribution of the throughput allocated to the different Waves instruments. Such an operating possibility is envisaged for the continuation of the mission ("autotune" mode), at the time of favourable events (passage at the level of the terrestrial shock, apogee...).

The choice of the 4 frequencies can also be modified by patches in the TNR or DPU.

4.10.2. Data transmitted by the DPU to the telemeter

Among the information transmitted to it by the TNR, the DPU transmits the following data to the telemetry system in the form of a general-purpose wave packet:

⁶⁷ In modes 0, 1, 2 and 3, only the first AGC value is significant. In mode 4, where both the TNRA and TNRB sub-receptors are read, both AGC values are significant.

⁶⁸ In reality, this data is superfluous for the DPU, which is already provided with the spectrum and f_p values. The reason for this is that if, during the course of the mission, it is envisaged to modify the choice of positions around f_p transmitted to the ground, this modification will be made by downloading at the TNR level; an equivalent modification would have been more difficult to envisage at the DPU level (see footnote in § 5-8-3).

⁶⁹ Such an option proves tricky in practice, given the insufficient number of points (TBC).

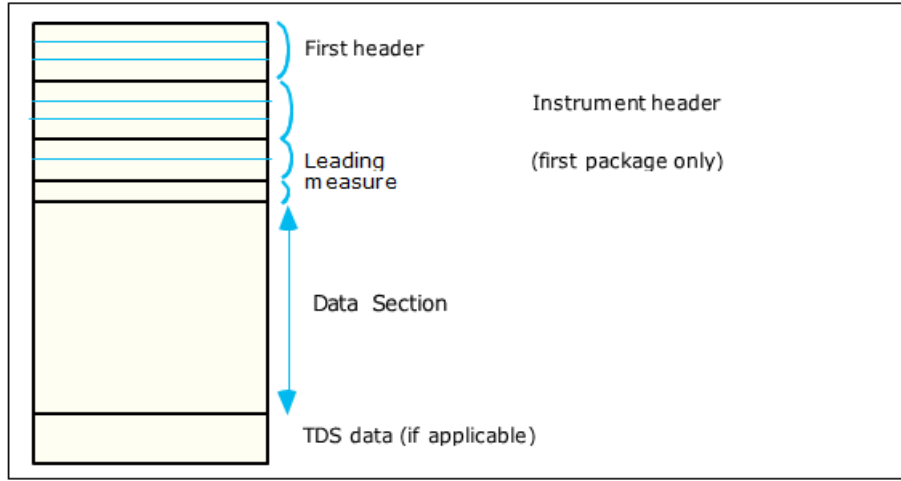


Fig. Structure of a TNR package

Header

First header

Byte 0	X X X X 0 0 0 0	Packet identifier (ID = 3)
	0 0 0 0 X 0 0 0	Is the measurement header present in this package?
	0 0 0 0 0 X 0 0	Is the instrument header present in this package
	0 0 0 0 0 0 X 0	Is this the last package of the event?
	0 0 0 0 0 0 0 X	Is this the last package of the event?
Byte 1	X X X X 0 0 0 0	What sub-type of package is this?
	0 0 0 0 0 0 X 0	Is the package header present in this package
Byte 2	0 0 0 0 0 0 0 X	Calculation of the position of the TDS data
	X X X X X X X X	

Instrument header (present only in the first package)

Byte 0	X X	fixed, ABCDE, or ACE
	X	tuning mode (0: no, 1: neural)
	X	state preservation in case of internal CAL
	X X	antenna (E_xE_y , E_xE_z , E_yE_x , E_yE_z)
Byte 1	X X X	band (A, B, C, D, E)
	X X X	mode (0 to 4)
	X X	integration time
Byte 2	X X X X X X X X	number of spectra in the event

Measurement header (present only in the first package)

Byte 0	X X X X X X X X	DPU mf
Byte 1	X X X X X X X X	DPU MF

Header Package

Byte 0	X X X X X X X X	package number in the event
--------	-----------------	-----------------------------

Data

The composition of the "DATA" part in the packet, following the header, depends on the DPU operating mode (Normal, Fast, Diagnostic) and the TNR operating mode (0, 1, 2, 3, 4), as shown in this table:

		<u>TNR modes</u>			
Modes of the DPU	NORMAL mode	<u>Mode 0.1</u> -16 spectrum values - 1 GAC value	<u>Mode 2,3</u> - 32 spectrum values - 1 GAC value	<u>Mode 4</u> - 2 x 16 spectrum values - 2 GAC values	
	Default rate	24 times/package	12 times/package		
	FAST mode	- 4 frequencies around f_p - 1 GAC value - 1 NN' composite - 16 last spectra values	- 4 frequencies around f_p - 1 GAC value - 1 NN' composite - 32 last spectra values	- 4 frequencies around f_p - 1 GAC value (or 2 AC) - 1 NN' composite - 2x16 last spectra values	
	pace	64 times/package (except for the last 16 or 32 spectra values and last AGC: 1 time/package)			
	DIAGNOSTIC mode	-16 spectrum values - 4 frequencies around f_p - 1 GAC value - 2 NN	- 32 spectrum values - 4 frequencies around f_p - 1 GAC value - 2 NN	- 2x16 spectrum values - 4 frequencies around f_p - 2 GAC values - 2 NN	
	pace	24 times/package	12 times/package		

We can see that we always have less than 431 words in this way.

Remarks

- The NN (Neural Network) symbol represents the 2 information f_p (channel number), and $v(f_p)$ (output value of the NN for this channel).
- The symbol NN' represents the 2 information f_p and $v(f_p)$ coded on 8 bits: f_p is coded on 5 bits, and we retain only the 3 MSB of $v(f_p)$.
- If we calculate for each case the number of words inserted in a packet, we always obtain a value lower than 431 (total number of words per packet). For example:
 - in normal mode of the DPU and 0.1 of the TNR: $(16+1) \times 24 = 408$
 - in fast mode of the DPU and 0.1 of the TNR: $(4+1+1) \times 64 + 16 = 400$

The rest of the available words in the packet are used by the packet header and by words in the TDS sub-experiment.

- The combination (DPU fast mode, TNR mode 4) is not very interesting. Indeed, in fast mode, the objective is not to acquire TNRA and TNRB data.
- Note that the diagnostic mode is the only mode that makes the spectra and the associated NN response available simultaneously. When downloading a new set of NN coefficients, the TNR instrument is put in diagnostic mode for some time.

4.11. Scanning of frequency bands

4.11.1. The different scanning modes

There are several possible modes of scanning the frequency bands:

- The ABCDE scan mode and the ACE scan mode.

- In ABCDE scanning, the frequency bands are scanned in the order A B C D E A B C D E A B ... For this mode, the DPU places 10 spectra in an event. For each band, the DPU collects one spectrum: to obtain these 10 spectra, the DPU scans the 5 frequency bands twice, which requires 10 analysis commands from the DPU to the TNR. The A, C and E bands would be enough to cover the whole frequency range of the TNR receiver. The B and D bands therefore provide redundant spectral information. The interval between two spectra is 7.36 s (LBR) and 3.68 s (HBR).
- The ACE scan consists in quickly scanning the complete frequency range of the TNR (4 kHz to 256 kHz) by scanning only the frequency bands A, C, E. Indeed, these 3 frequency bands alone cover the complete frequency range [4 kHz, 256 kHz] of the TNR receiver. For this mode, the DPU inserts 12 spectra into an event. For each band, the DPU collects one spectrum: to obtain the 12 spectra, the DPU scans the 3 frequency bands 4 times, which requires 12 analysis commands from the DPU to the TNR. The A, C and E band path allows to cover the whole frequency range of the TNR instrument. It is therefore the more efficient of the two scanning modes. The interval between two spectra is 4.42 s (LBR) and 2.21 s (HBR).

- Fixed band mode: in this mode, the TNR receiver remains positioned on one of the 5 possible bands. The advantage of this mode is that it gives f_p with a high time resolution. On the other hand, this mode carries the obvious risk that the chosen frequency band does not contain f_p . The positioning in this mode results from a remote control or from the tracking mode.

- Tracking mode (or NN control or "autotune"). In this mode, the NN drives the receiver, in the sense that the DPU decides on the frequency band in which the TNR receiver is positioned at a given time, based on the results of the NN. This mode implements both the fixed band mode and the ABCDE and ACE scan modes.

4.11.2. The pursuit mode

4.11.2.1. Principle

One of the objectives of the TNR instrument is to test the possibility of tracking the position of the plasma frequency over time. To do this, it is necessary to remain positioned in the corresponding frequency band as often as possible and in a reliable manner. The best frequency band at a given time is the one for which the plasma frequency is well centered in this band, with sufficient spectral points on both sides of f_p . In particular, it should be avoided that the frequency band in effect is such that the plasma frequency is at one end of it. If this is the case, a decision must be made to change the band. The purpose of the plasma frequency tracking algorithm resident in the DPU is to control the TNR instrument to meet this requirement.

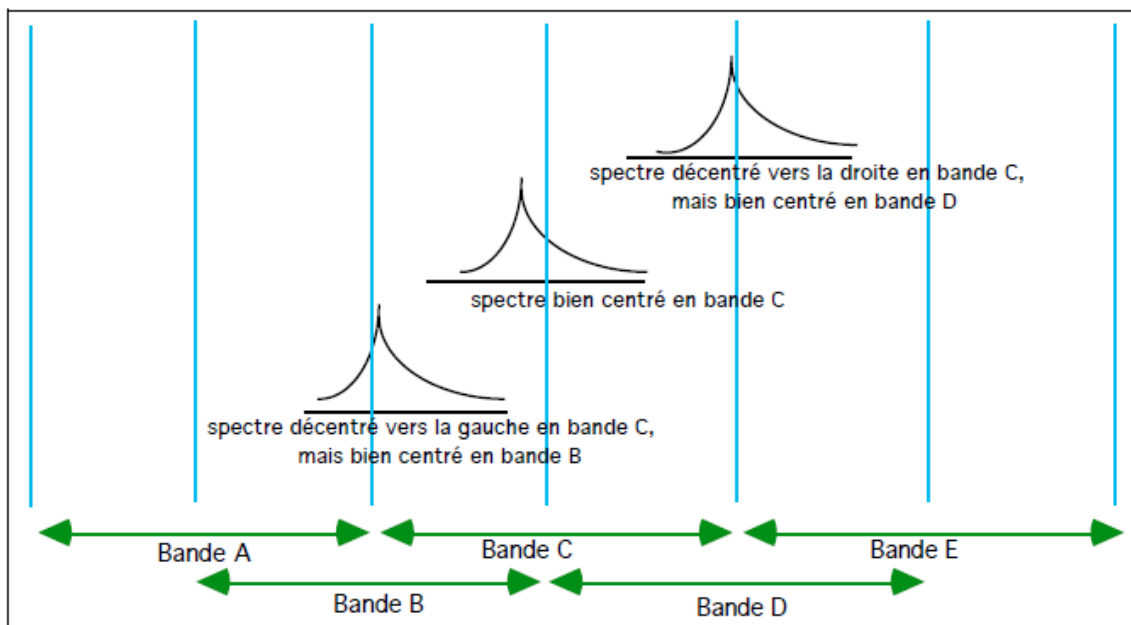


Fig. Adaptation of the frequency band to the current plasma frequency.

4.11.2.2. Course of action

The precise flow of the f_p tracking algorithm can be found in the DPU program written by K. Goetz in 32-bit NS assembler. A flowchart describing this algorithm is given below⁷⁰.

An event groups a number of spectra: 12 in default mode with an ACE scan, 10 in ABCDE scan mode. Every multiple of events, a function is called. This function has as argument the search mode (neural_Network_to_tune) or the fixed mode (fixed_Mode).

Neural network to tune" mode

This mode is used in two circumstances: the first time, to find the position of the plasma frequency, or afterwards, to find it again, when the instrument has lost it. The DPU starts by scanning the frequency bands (ABCDE or ACE) and calculates the sum_centre_RN_i values (i=1,..,5) which are the scores obtained in the central parts of the 5 frequency bands. The limits of these central parts of the frequency bands are defined beforehand in an arbitrary way:

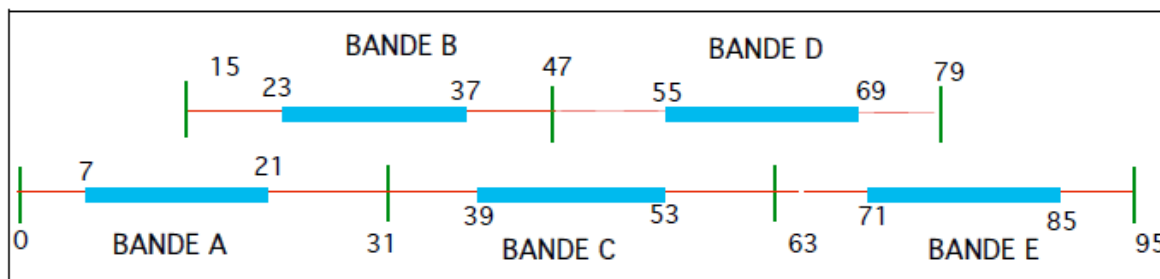


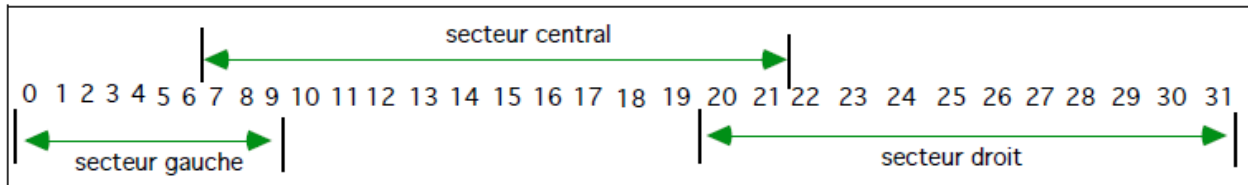
Fig. central parts

⁷⁰ In fact, the algorithm can also take into account information from 3D Plasma and SWE (TBC).

Then it determines the highest of these 5 values. If this value is higher than a predefined threshold (threshold_RN_to_tune), the DPU forces the TNR to stay on this frequency band (switch to "fixed tune" mode). Otherwise, the DPU starts scanning the bands again.

Fixed tune mode

The 32 channels of the current frequency band are divided into 3 sectors: left (channel 0 to 9), center (channel 7 to 21), right (channel 19 to 31). There is a slight overlap from one sector to the next.



The DPU calculates the sum of the scores of the NN (on a given number 10: AC of successive results of the NN) in the central sector (sum_centre_RN). If this sum is higher than a predefined threshold, one remains positioned in this band. Otherwise, we compute the sum of the scores in the left sector (sum_left_RN). If this sum is higher than a predefined threshold, we position ourselves on the previous adjacent band (except if we are already in band A, in which case we return to search mode). Otherwise, the sum in the right sector is calculated (sum_right_RN). If this sum is higher than a predefined threshold, we switch to the next adjacent band (except if we are already in band E, in which case we switch back to search mode). Otherwise, it means that no sum, neither in the center, nor on the left, nor on the right, reaches the threshold necessary to stay in a band, or that you change band: you then go into "Neural Network to tune" mode.

Remarks

- The sums (the values νf given by the NN, i.e. the quality indices, are added for each channel f) are calculated for $NSE \times NE$ spectra, where NSE = number of spectra per event (default value: 10 in ABCDE and 12 in ACE) and NE = number of events taken into account (default value:) for a DPU decision The thresholds used are as follows:

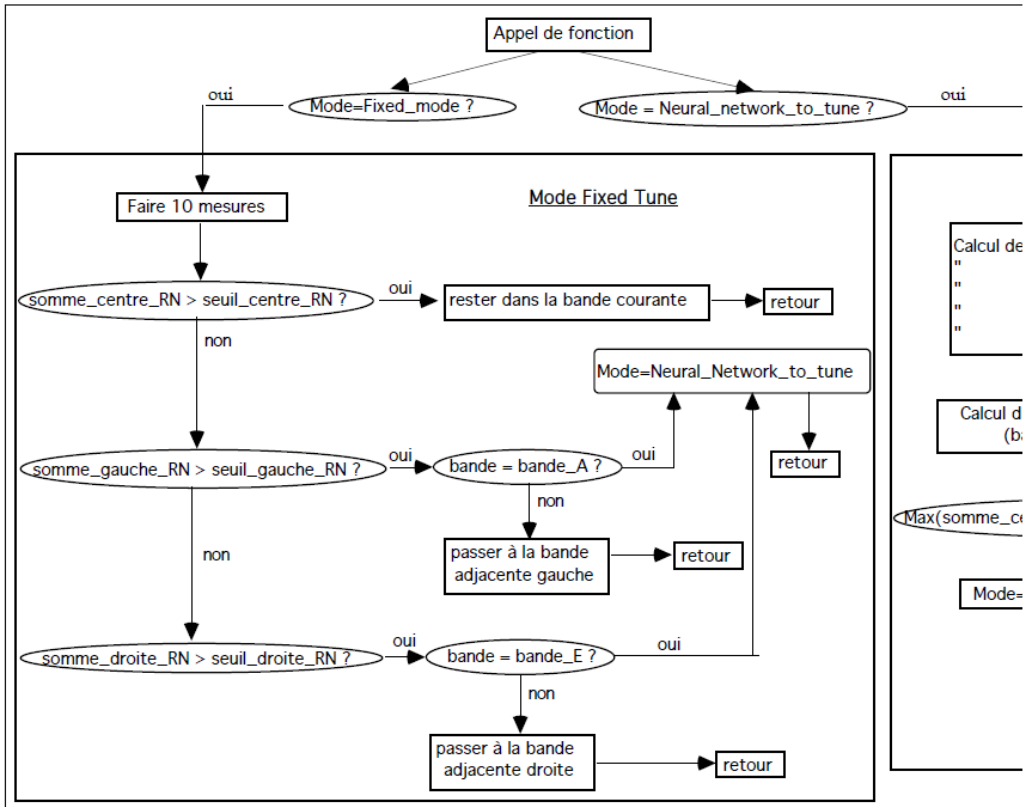
threshold_right_RN: $NSE \times NE \times \text{default value}$
 threshold_center_RN: $NSE \times NE \times \text{default value}$
 threshold_left_RN: $NSE \times NE \times \text{default value}$

- To avoid being misled by inaccurate NN results and remaining in an inappropriate frequency band, i.e. not containing the plasma frequency, the DPU periodically commands a switch to the honesty factor. This results in a moderate loss of spectra. This disconnection occurs every 100 events, i.e., in LBR, $100 \times 10 \times 1.472 = 1472$ seconds = about 25 minutes (in ABCDE sweep), or , $100 \times 12 \times 1.472 \text{ s} =$ about 30 minutes (in ACE sweep), and twice less in HBR.
- After the central sector, the left sector is examined first, and not the right sector. Indeed, disturbances (such as type III bursts) appear to the right of f_p and we therefore prefer in the algorithm to favour the choice of the left sector.

- Since the function is called every event multiple⁷¹, it is only possible to change modes at these times: a command (e.g. change band) from DPU to TNR can only be given every event multiple. An event gathers 10 or 12 spectra in normal mode and 64 in fast mode. In normal mode, taking into account the integration time which is nominally 1.472s (LBR) or 0.736s (HBR), this results in a time between two function calls of about 15 or 18 seconds (LBR) and 7.5 or 9 seconds (HBR). Various problems may arise from this delay, for example if the plasma frequency increases by changing bands just after this limit. However, a very intense shock could only introduce a multiplication of the density by a factor of about 4, and thus by a factor of 2 in frequency⁷². Ultimately, this rate of function call should not prove to be very limiting.
- As of today, the tracking mode has only been marginally implemented for the operational purpose of tracking the plasma line and thus changing bands as it evolves. A new set of NN coefficients was downloaded on 27 June 1995, allowing the tracking mode to be tested for 11 days, from 27 June to 7 July 1995. The rest of the time, the TNR instrument operates in scan mode (ABCDE and most often ACE), as can be seen from the summary plots. In this case, the DPU does not take into account the information provided by the NN.
- The DPU diagnostic mode is the only mode that makes the spectra and the associated NN response available simultaneously. When downloading a new set of NN coefficients, the TNR instrument is put in diagnostic mode for some time. This mode therefore allows the TNR results to be tested in real, non-simulated operation of the instrument.
- The determination of f_p can be done in possible combination with the electron density information measured by the SWE and 3D Plasma experiments onboard the spacecraft. The 3D Plasma experiment provides an electron density measurement once per satellite rotation (3 seconds). The SWE Plasma experiment provides a TBW electron density measurement. This capability is part of the software. SWE and 3D Plasma are not used at this time. Should one decide to use this information, the determination of f_p is done according to a weighting of: $\langle \text{SWE} \rangle$, $\langle \text{3D Plasma} \rangle$ and $\langle \text{TNR} \rangle$, these 3 quantities being 3-bit numbers estimating f_p , provided by the 3 experiments. In this regard, there is the problem of calibration of SWE and 3D Plasma data. The DPU has a table to translate the values provided to it by the other two sub-experiments. (AC)

⁷¹ By default, at the present time, the function is called up once every event (to be confirmed).

⁷² Note that other phenomena, such as discontinuities, can generate a significant variation in density.



The list of ICP remote controls for the TNR instrument is as follows:

3. TNR

3.1. Mode

3.2. Antenna

3.2.1. ExEy

3.2.2. ExEz

3.2.3. EyEz

3.2.4. EyEx

3.3. Reset

3.4. Integration_Time

3.4.1. A_1472ms

3.4.2. B_736ms

3.4.3. C_368ms

3.4.4. D_184ms

3.5. . State

3.5.1. Fixed_Tune

3.5.1.1. A_8kHz

3.5.1.2. B_16kHz

3.5.1.3. C_32kHz

3.5.1.4. D_64kHz

3.5.1.5. E_128kHz

3.5.2. ABCDE

3.5.3. ACE

3.5.4. Auto_Tune

3.5.4.1. Off

3.5.4.2. NN

3.5.4.3. Boink

3.5.4.4. Event/Decision

3.5.4.5. Honesty

3.6. . Spectra(num/ev)

3.8. Immediate

3.8.1. Fixed_Tune

3.8.1.1. A_8kHz

3.8.1.2. B_16kHz

3.8.1.3. C_32kHz

3.8.1.4. D_64kHz

3.8.1.5. E_128kHz

3.8.2. Antenna

3.8.2.1. ExEy

3.8.2.2. ExEz

3.8.2.3. EyEz

3.8.2.4. EyEx

3.8.3. Integration_Time

3.8.3.1. A_1472ms

3.8.3.2. B_736ms

3.8.3.3. C_368ms

3.8.3.4. D_184ms

3.8.4. Mode

3.8.5. On

3.8.6. Off

3.9. ML/MD

3.9.1. Hex_command(14bits)

3.9.2. Load

3.9.3. Start_Dump

3.9.4. Byte_Dump

3.9.5. Trio_Dump

3.9.6. On

3.9.7. Off

3.9.8. Abort

3.10. TM_mode

3.10.1. Diagnosis

3.10.2. Normal

3.10.3. Fast

6. Reset_DPU

6.1. Warm

6.2. Cold